

A parallel space-time p -adaptive discontinuous Galerkin method for nonlinear acoustics

Daniele Corallo, Pascal Lehner, Christian Wieners

Abstract

In this paper, we introduce and analyze a space-time p -adaptive discontinuous Galerkin method for nonlinear acoustics.

We first present the underlying mathematical model, which is based on a recently derived formulation involving, in particular, only first order in time derivatives. We then propose a space-time discontinuous Galerkin discretization of this model, combining a symmetric Friedrichs systems discretization for symmetric hyperbolic systems with an interior penalty discretization for damping terms. The resulting nonlinear system is solved using Newton's method.

Next, we present a well-posedness analysis of the discrete problem. The analysis begins with a linearized system, for which stability is shown. Using a fixed point argument, these results are extended to the fully discrete nonlinear system, yielding a priori error estimates in a natural discontinuous Galerkin norm.

Finally, we present numerical experiments demonstrating the parallel solvability of the space-time formulation and the effectiveness of p -adaptivity. The results confirm the theoretical convergence rates and show that adaptive refinement can reduce the number of degrees of freedom required to accurately approximate selected goal functionals. Moreover, the experiments demonstrate that the model reproduces characteristic phenomena of nonlinear acoustics, such as harmonic generation, thereby validating the proposed model.

1 Introduction

Efficient numerical methods for nonlinear acoustics are essential across various scientific and engineering disciplines. In engineering, nonlinear acoustic phenomena play a critical role in nondestructive material testing [16], underwater acoustics [6] and supersonic sources [36]. From a medical perspective, accurately modeling the propagation of nonlinear acoustic waves through biological tissue is essential for both diagnostic and therapeutic applications, including medical imaging, tissue ablation, lithotripsy, and targeted drug delivery, see [35].

The simulation of nonlinear acoustics is often challenging due to the interplay between high frequency wave propagation and nonlinear effects. Many classical models, such as Westervelt's [39] and Kuznetsov's equation [26], involve second order time derivatives that act on nonlinear terms. This significantly complicates the design of stable and efficient numerical methods. Moreover, a key difficulty lies in resolving the nonlinearities in the presence of steep gradients or shock like structures that often emerge during wave propagation, see [20] for more details on the physics of nonlinear acoustics.

Numerous numerical methods have been proposed in the literature to address these challenges. Here, we focus on works that include an error analysis of a finite element method. For the Westervelt equation, semi-discrete finite element approximations with optimal error estimates have been studied in [32], while semi-discrete discontinuous Galerkin (DG) methods have been analyzed in [1]. A time stepping DG approach using conforming spatial elements is presented in [19], and a hybridizable DG formulation is discussed in [17]. Efficient time integration techniques based on operator splitting are introduced in [23]. For the Kuznetsov equation, a mixed finite element analysis is provided in [17]. Robust error estimates with respect to the damping parameter for a mixed method are derived in [13], and coupling with elastic wave equations is addressed in [31].

A model for nonlinear acoustics using only first order time derivatives with a structure preserving discretization and conforming elements is developed in [14], with additional insights presented in [3]. Other numerical approaches, such as finite volume and finite difference methods, have also been explored, though often without convergence analysis. A finite volume method for Westervelt's equation has been investigated in, for example, [38], while a finite difference method has been studied in [33].

In this paper, we propose a space-time DG method for a nonlinear acoustic model closely related to Kuznetsov's equation, derived in [22]. The key distinction of this formulation to classical models is the use of only first order in time derivatives, and that the nonlinear terms only involve spatial derivatives. To the best of our knowledge, this work represents the first application of a space-time DG method to nonlinear acoustics. The motivation for considering space-time methods lies in their intrinsic suitability for adaptive refinement, parallel implementation, and inverse problems. Advanced space-time DG methods have been devolved for wave equations in e.g. [2, 8, 24, 27, 30], for parabolic problems in [7, 18], and for Navier-Stokes equations in [25, 34, 37]. We emphasize that this list of references is by no means exhaustive.

The remainder of the paper is organized as follows. In section 2, we introduce the continuous mathematical model and present the space-time DG discretization analyzed in this work. Section 3 is devoted to the discrete well-posedness analysis of a linearized system. In section 4, these results are extended to the fully nonlinear discrete problem, yielding well-posedness and a priori error estimates for the proposed method. Numerical experiments validating the efficiency and possibility of a p -adaptive and parallel implementation are presented in section 5. Finally, concluding remarks and directions for future research are given in section 6.

2 First order in time model

In this section, we present the continuous model and its space-time DG discretization considered in this work. The derivation of this first order in time model is based on the standard assumption of small amplitude wave propagation and follows a methodology similar to that used in the derivation of Kuznetsov's equation. A key difference, however, is that one avoids taking additional derivatives of the reduced Navier–Stokes system, which are employed in the Kuznetsov or Westervelt formulation to further simplify the equations. For a detailed derivation, we refer the reader to [22].

2.1 Continuous model

Let $\Omega \subset \mathbb{R}^d$ be an open, bounded space domain with dimension $d \in \{2, 3\}$, and let $\Gamma := \partial\Omega$ denote the boundary of Ω , which is assumed to be Lipschitz. Furthermore, let $I := (0, T) \subset \mathbb{R}$ denote a time interval with final time $T > 0$, and define the corresponding space-time domain $Q := I \times \Omega$. The model is governed by parameters satisfying

$$\alpha, \beta, \gamma, \delta, \varepsilon, \zeta, \eta, \theta > 0, \gamma \neq \delta,$$

and takes the form

$$\begin{aligned} \alpha \partial_t p + \nabla \cdot \mathbf{v} - \beta \Delta p + \gamma p \nabla \cdot \mathbf{v} + \delta \nabla p \cdot \mathbf{v} &= p_S & \text{in } Q \\ \varepsilon \partial_t \mathbf{v} + \nabla p - \zeta \Delta \mathbf{v} + \frac{1}{2} \nabla (\eta \mathbf{v}^2 - \theta p^2) &= \mathbf{v}_S & \text{in } Q \\ p &= p_0, \quad \mathbf{v} = \mathbf{v}_0 & \text{on } \{0\} \times \Omega \\ p &= p_D, \quad \mathbf{v} = \mathbf{v}_D & \text{on } I \times \Gamma_D \\ \beta \nabla p \cdot \mathbf{n} &= p_N, \quad \mathbf{v} = \mathbf{v}_N & \text{on } I \times \Gamma_N \end{aligned} \tag{1}$$

with $\Gamma_D \cup \Gamma_N = \Gamma$, where $\Gamma_D \cap \Gamma_N = \emptyset$, and Γ_D has positive $(d-1)$ -dimensional Lebesgue measure. In this model of nonlinear acoustics $p : Q \rightarrow \mathbb{R}$ can be understood as the fluctuation of pressure and $\mathbf{v} : Q \rightarrow \mathbb{R}^d$ as the fluctuation of the velocity field, respectively, cf. [22, Section 2] for details. By \mathbf{n} we denote the outer unit normal vector on $\partial\Omega$ and \cdot^\top means transposition of a vector or matrix. We write $\mathbf{v}^2 := \mathbf{v} \cdot \mathbf{v}$ for the squared norm of a vector, $\nabla := (\partial_{x_1}, \dots, \partial_{x_d})^\top$ for the vector of spatial partial derivatives, $\Delta := \nabla \cdot \nabla$ for the Laplace operator, which acts component wise on vector fields, and ∇ for the Jacobian matrix of a vector field.

In order to simplify notation, we rewrite equation (1) with $u = (u_p, u_\mathbf{v})^\top = (p, \mathbf{v})^\top \in \mathbb{R}^{1+d}$ as

$$\begin{aligned} (M \partial_t + A - D \Delta) u + N(u, u) &= f & \text{in } Q \\ u &= u_0 & \text{on } \{0\} \times \Omega \\ \mathcal{B}_D u &= u_D & \text{on } I \times \Gamma_D \\ \mathcal{B}_N u &= u_N & \text{on } I \times \Gamma_N \end{aligned} \tag{2}$$

with matrices $M := \text{diag}(\alpha, \varepsilon, \dots, \varepsilon)$, $D := \text{diag}(\beta, \zeta, \dots, \zeta) \in \mathbb{R}^{(1+d) \times (1+d)}$, first order differential operators

$$A u := \begin{pmatrix} \nabla \cdot u_\mathbf{v} \\ \nabla u_p \end{pmatrix}, \quad N(u, z) := \begin{pmatrix} \gamma z_p \nabla \cdot u_\mathbf{v} + \delta \nabla u_p \cdot z_\mathbf{v} \\ \eta (\nabla u_\mathbf{v})^\top z_\mathbf{v} - \theta z_p \nabla u_p \end{pmatrix},$$

boundary operators $\mathcal{B}_D u = u$, $\mathcal{B}_N u = (\nabla u_p \cdot \mathbf{n}, u_{\mathbf{v}})^\top$, and given data

$$\begin{aligned} f &:= (p_S, \mathbf{v}_S)^\top \in L^2(Q; \mathbb{R}^{1+d}), \\ u_0 &:= (p_0, \mathbf{v}_0)^\top \in H^1(\Omega; \mathbb{R}^{1+d}), \\ u_D &:= (p_D, \mathbf{v}_D)^\top \in H^1(0, T; H^{\frac{3}{2}}(\Gamma_D; \mathbb{R}^{1+d})), \\ u_N &:= (p_N, \mathbf{v}_N)^\top \in H^1(0, T; H^{\frac{1}{2}}(\Gamma_N) \times H^{\frac{3}{2}}(\Gamma_N; \mathbb{R}^d)). \end{aligned} \tag{3}$$

In [22, 29] it is shown that equation (2) is well posed for any $T > 0$ with

$$u \in U := H^1(0, T; L^2(\Omega; \mathbb{R}^{1+d})) \cap L^2(0, T; H^2(\Omega; \mathbb{R}^{1+d}))$$

assuming that $\Gamma_D = \partial\Omega$ or $\Gamma_N = \partial\Omega$ is C^2 -regular, and that the data (3) are sufficiently small with respect to the corresponding norms. Note that in our analysis the case $\Gamma_N = \partial\Omega$ is not included.

This is established as follows. Writing equation (2) as

$$G(u) := Lu - D\Delta u + N(u, u) - f = 0 \tag{4}$$

with $L := M\partial_t + A$, it is shown in [22, 29] that there exists an $r > 0$ such that Newton's method with starting value 0 converges to a unique $u \in B_r^U(0)$ such that $G(u) = 0$. Here, for any normed space X , $r > 0$ and $x \in X$ we denote the open ball with radius r centered at x as $B_r^X(x)$. In the analysis, it becomes necessary to compute the Fréchet derivative of G in U at \tilde{u} . Owing to the bilinearity of $N(\cdot, \cdot)$ and the linearity of all other operators in G , one can demonstrate through suitable estimates on $N(\cdot, \cdot)$, that G is Fréchet differentiable in U . Then, Newton's method requires the linear system

$$\begin{aligned} (L - D\Delta)u + N(u, \tilde{u}) + N(\tilde{u}, u) &= f^{\tilde{u}} && \text{in } Q \\ u = u_0 && \text{on } \{0\} \times \Omega \\ \mathcal{B}_D u = u_D && \text{on } I \times \Gamma_D \\ \mathcal{B}_N u = u_N && \text{on } I \times \Gamma_N, \end{aligned} \tag{5}$$

to be solved in each iteration, where in the context of Newton's method $f^{\tilde{u}}$ plays the role of a residual and $\tilde{u} \in U$ denotes the previous iterate. To establish global in time well-posedness of equation (5), the data (3) and $f^{\tilde{u}}$ are assumed to be small enough. Once this is proven, the Newton-Kantorovich Theorem, see Lemma 4.1 below, can be applied to G . This gives global in time well-posedness of equation (2), if the data (3) are sufficiently small. For showing the well-posedness of the discrete system, we follow a similar strategy, see section 4.

2.2 Space-time discretization

To begin, we introduce some notation. Let $S \subset \mathbb{R}^s$ be Lipschitz with $s \in \mathbb{N}$. We use the abbreviation $L^2 = L^2(S) = L^2(S; \mathbb{R}^i)$ with $i \in \mathbb{N}$ when the context is clear. The standard L^2 inner product of two functions $f, g \in L^2(S; \mathbb{R}^i)$ is given by $(f, g)_S := \int_S f \cdot g \, d\sigma$, where σ is a measure on S . If f, g are matrix-valued, $f \cdot g$ corresponds to the Frobenius inner product. Let $k \in \mathbb{N}$ denote the number of time points of the considered discretization. For given time points $0 =: t_0 < t_1 < \dots < t_{k-1} < t_k := T$, we define the following time intervals and time step sizes for $j \in \{1, \dots, k\}$.

$$I_j := (t_{j-1}, t_j), \quad I_h := \bigcup_{j=1}^k I_j \subset I, \quad \partial I_h := \bigcup_{j=0}^k \{t_j\}, \quad \tau_j := t_j - t_{j-1}, \quad \tau := \max_{j \in \{1, \dots, k\}} \tau_j.$$

In this paper, we assume a quasi-uniform time discretization, i.e., $\tau_j \in [C_{sr}\tau, \tau]$ for all $j \in \{1, \dots, k\}$ with a shape regularity constant $C_{sr} \in (0, 1]$ independent of k and j .

For the spatial discretization, let \mathcal{K}_h be a conforming shape-regular mesh of Ω so that $\Omega_h := \bigcup_{K \in \mathcal{K}_h} K$ is a decomposition of Ω into open non overlapping space cells $K \subset \Omega$. We denote spacial mesh sizes as $h_K := \text{diam}(K)$ and $h := \max_{K \in \mathcal{K}_h} h_K$.

For simplicity, we consider only tensor-product space-time meshes in this article. To obtain a tensor-product mesh of Q , we define

$$Q_h := I_h \times \Omega_h = \bigcup_{R \in \mathcal{R}_h} R \text{ with } \mathcal{R}_h := \{R \subset Q : \exists j \in \{1, \dots, k\}, \exists K \in \mathcal{K}_h : R = I_j \times K\},$$

such that $\overline{Q_h} = \overline{Q}$. We assume that the mesh sizes in time and space are well balanced satisfying for some $\omega \in [1, \infty)$

$$h^\omega \leq c_r \tau \leq h < 1, \quad (6)$$

where $c_r > 0$ is a reference velocity yielding the bound $\tau^{-1} \leq c_r h^{-\omega}$.

Element boundaries

We denote by \mathcal{F}_K the set of faces of a space element $K \in \mathcal{K}_h$, and define the set of all faces as $\mathcal{F}_h := \bigcup_{K \in \mathcal{K}_h} \mathcal{F}_K$, where $h_F = \text{diam}(F)$ for $F \in \mathcal{F}_h$. The space skeleton is then given by $\partial\Omega_h = \overline{\bigcup_{F \in \mathcal{F}_h} F}$, and the corresponding space-time skeleton is $\partial Q_h = \partial I_h \times \overline{\Omega} \cup \overline{I} \times \partial\Omega_h$.

We distinguish between boundary faces $\mathcal{F}_h^{\text{ext}} := \{F \in \mathcal{F}_h : F \subset \partial\Omega\}$ and interior faces $\mathcal{F}_h^{\text{int}} := \mathcal{F}_h \setminus \mathcal{F}_h^{\text{ext}}$. Additionally, we define Dirichlet faces as $\mathcal{F}_h^D := \{F \in \mathcal{F}_h : F \subset \Gamma_D\}$ and Neumann faces as $\mathcal{F}_h^N := \{F \in \mathcal{F}_h : F \subset \Gamma_N\}$. We assume that the mesh \mathcal{K}_h is such that $\mathcal{F}_h^{\text{ext}} = \mathcal{F}_h^D \cup \mathcal{F}_h^N$ disjointly with $\mathcal{F}_h^D \subset \Gamma_D$, $\mathcal{F}_h^N \subset \Gamma_N$ such that $\overline{\bigcup_{F \in \mathcal{F}_h^D} F} = \Gamma_D$ and $\overline{\bigcup_{F \in \mathcal{F}_h^N} F} = \Gamma_N$. Furthermore, we require that the $(d-1)$ -dimensional Lebesgue measure of \mathcal{F}_h^D is positive.

If an interior face $F \in \mathcal{F}_h^{\text{int}}$ is contained in $K \in \mathcal{K}_h$, we write K_F for the unique neighbor cell such that $F = \partial K \cap \partial K_F$. For an exterior face $F \in \mathcal{F}_h^{\text{ext}} \subset K \in \mathcal{K}_h$, we set $K_F = K$. Each element $K \in \mathcal{K}_h$ is assigned the outer normal vector \mathbf{n}_K of ∂K .

Approximation spaces

Let $i, s \in \mathbb{N}$. We define the space of polynomials $\mathcal{P}(S; \mathbb{R}^i) := \bigcup_{\deg=0}^{\infty} \mathcal{P}^{\deg}(S; \mathbb{R}^i)$, where $\mathcal{P}^{\deg}(S; \mathbb{R}^i)$ is the set of polynomials $\varphi : S \rightarrow \mathbb{R}^i$ with degree less or equal then $\deg \in \mathbb{N}_0$ for any set $S \subset \mathbb{R}^s$. The approximation spaces considered here are broken polynomial spaces, namely, subsets of

$$\mathcal{P}_h(S; \mathbb{R}^i) := \{\varphi \in L^2(S; \mathbb{R}^i) : \varphi|_S \in \mathcal{P}(S_h; \mathbb{R}^i) \ \forall S_h \in \mathcal{S}_h\},$$

where \mathcal{S}_h is some mesh of S .

To construct space-time tensor product broken polynomial spaces, we assign polynomial degrees $p_R \in \mathbb{N}_0$ in time and $q_R \in \mathbb{N}_0$ in space to every space-time cell $R \in \mathcal{R}_h$. This results in the discontinuous finite element space

$$Z_h := \{\varphi \in L^2(Q; \mathbb{R}^{1+d}) : \varphi|_{R=I_j \times K} \in \mathcal{P}^{p_R}(I_j; \mathbb{R}^{1+d}) \otimes \mathcal{P}^{q_R}(K; \mathbb{R}^{1+d}) \ \forall R \in \mathcal{R}_h\}, \quad (7)$$

which is used in this paper. Here, \otimes denotes the tensor product between vector spaces.

Boundary operators

Let $w \in (H^1(I; L^2(\Omega; \mathbb{R}^i)) \cap L^2(I; H^1(\Omega; \mathbb{R}^i))) \cup \mathcal{P}_h(Q, \mathbb{R}^i)$ with $i \in \mathbb{N} \cup (\mathbb{N} \times \mathbb{N})$ be such that traces in time and space of w exist on \mathcal{R}_h . For $K \in \mathcal{K}_h$ and $j \in \{1, \dots, k\}$, we define $w_j := w|_{I_j}$ and $w_K := w|_K$, where the evaluation of these expressions at boundary points is understood in the sense of traces. In particular, this gives

$$w_j(t_j) = \lim_{t \rightarrow t_j^+} w_j(t), \quad w_j(t_{j-1}) = \lim_{t \rightarrow t_{j-1}^-} w_j(t),$$

if the limits exist.

Let $K \in \mathcal{K}_h$ be a space cell, $F \in \mathcal{F}_K \cap \mathcal{F}_h^{\text{int}}$, K_F the neighboring cell. We define the (space) jump at F with respect to K as

$$[w]_{F,K}(t, x) := w_{K_F}(t, x) - w_K(t, x) \quad x \in F, t \in I.$$

The jump with respect to time is defined for each $j = 1, \dots, k-1$ as

$$[w]_j(x) := w_{j+1}(t_j, x) - w_j(t_j, x) \quad x \in \Omega,$$

and for the boundary cases $j = 0, k$, we set $[w]_0(\cdot) := w(t_0, \cdot)$, $[w]_k(\cdot) := -w(t_k, \cdot)$.

Additionally, we use the notion of a (space) jump at faces $F \in \mathcal{F}_h$ without a particular reference cell. For this, we define \mathbf{n}_F as the unit outer normal vector of F . If $F \in \mathcal{F}_h^{\text{ext}}$, \mathbf{n}_F is taken to have the same orientation as \mathbf{n}_K with $F \subset K$. Otherwise, the orientation of \mathbf{n}_F may be chosen arbitrarily. Let F and F_1 be adjacent faces with $F \subset K, F_1 \subset K_1$. The (space) jump at F is defined as

$$[w]_F(t, x) := w_K(x, t) - w_{K_1}(x, t) \quad x \in F \cap F_1, t \in I$$

and the (space) average at F is

$$\langle w \rangle_F(t, x) := \frac{1}{2} (w_K(x, t) + w_{K_1}(x, t)) \quad x \in F \cap F_1, t \in I.$$

On boundary faces $F \in \mathcal{F}_h^{\text{ext}}$, we set $[w]_F = \langle w \rangle_F = w|_F$.

2.3 Discontinuous Galerkin scheme

We now introduce the DG scheme for equations (2) and (5) considered in this article. DG space-time discretizations of $M\partial_t + A$ can be framed within the theory of symmetric Friedrichs systems, see, e.g., [10, Chapter 7]. In this context, we build upon the primal formulation of a Friedrichs system and then add terms corresponding to an interior penalty method for the Laplace operator $-\Delta$, see, e.g., [10, 11], along with nonlinear volume terms.

For convenience, we do not change the notation of differential operators, when applied to globally discontinuous functions. In these cases, we mean the broken operator, which is defined piecewise on each (space-time) cell.

Symmetric Friedrichs system

To discretize $\partial_t M + A$, as in [12], we consider the following bilinear forms defined on $Z_h \times Z_h$, cf. (7),

$$m_h(u_h, z_h) := \sum_{j=1}^k \left(\int_{t_{j-1}}^{t_j} (M\partial_t u_h, z_h)_{\Omega_h} dt + (M[u_h]_{j-1}, z_{h,j}(t_{j-1}))_{\Omega_h} \right)$$

and

$$a_h(u_h, z_h) := \int_0^T \sum_{K \in \mathcal{K}_h} \left((Au_h, z_h)_K + \sum_{F \in \mathcal{F}_K} (A_{\mathbf{n}_K}^{\text{up}} [u_h]_{F,K}, z_{h,K})_F \right) dt, \quad (8)$$

where

$$A_{\mathbf{n}_K}^{\text{up}} := \frac{1}{2} \begin{pmatrix} -\sqrt{\frac{\alpha}{\varepsilon}} & \mathbf{n}_K^\top \\ \mathbf{n}_K & -\sqrt{\frac{\varepsilon}{\alpha}} \mathbf{n}_K \mathbf{n}_K^\top \end{pmatrix} \in \mathbb{R}^{(1+d) \times (1+d)} \quad (9)$$

is related to an upwind flux based on solving local Riemann problems, see section A for the derivation of $A_{\mathbf{n}_K}^{\text{up}}$ for $d = 2$.

In (8), the jump terms $[u_h]_{F,K}$ are not defined for boundary faces $F \subset \Gamma$. To treat the boundary conditions correctly, we adopt the following convention

$$\begin{cases} [u_h]_{F,K} := -u_h & \text{for } F \in \Gamma_D, \\ [u_h]_{F,K} := -2(0, v_h)^\top & \text{for } F \in \Gamma_N \end{cases} \quad (10)$$

with $u_h = (p_h, v_h)^\top$.

As it is shown in [8] (and also is proven in section A), the definition (10) ensures the bounds

$$c_A \int_0^T \|A_{\mathbf{n}}[z_h]\|_{L^2(\partial\Omega_h)}^2 dt \leq a_h(z_h, z_h) \leq C_A \int_0^T \|A_{\mathbf{n}}[z_h]\|_{L^2(\partial\Omega_h)}^2 dt \quad \forall z_h \in Z_h \quad (11)$$

with

$$\|A_{\mathbf{n}}[z_h](t)\|_{L^2(\partial\Omega_h)} := \left(\sum_{K \in \mathcal{K}_h} \sum_{F \in \mathcal{F}_K} \|A_{\mathbf{n}}[z_h](t)\|_F \right)^{\frac{1}{2}}, \quad A_{\mathbf{n}_K} := \begin{pmatrix} 0 & \mathbf{n}_K^\top \\ \mathbf{n}_K & 0 \end{pmatrix},$$

where $c_A, C_A > 0$ only depend on α and ε and $A_{\mathbf{n}_K}^{\text{up}}$ is defined in (9).

Interior penalty method and nonlinear terms

To discretize the Laplacian terms $-D\Delta$, we use the interior penalty method, see, for example, [10, 11] and the references therein. The associated bilinear form is given by

$$d_h(u_h, z_h) := (D\mathbf{\nabla} u_h, \mathbf{\nabla} z_h)_{Q_h} + \int_0^T \rho_h^\Theta(u_h, z_h) dt \quad (12)$$

with

$$\begin{aligned} \rho_h^\Theta(u_h, z_h) := & \beta \sum_{F \in \mathcal{F}_h \setminus \mathcal{F}_h^N} -\Theta([p_h]_F, \langle \nabla q_h \rangle_F \cdot \mathbf{n}_F)_F - (\langle \nabla p_h \rangle_F \cdot \mathbf{n}_F, [q_h]_F)_F + \sigma_{F,h}([p_h]_F, [q_h]_F)_F \\ & + \zeta \sum_{F \in \mathcal{F}_h} -\Theta([v_h]_F, \langle \nabla w_h \rangle_F \mathbf{n}_F)_F - (\langle \nabla v \rangle_F \mathbf{n}_F, [w_h]_F)_F + \sigma_{F,h}([v_h]_F, [w_h]_F)_F, \end{aligned}$$

using $z_h = (q_h, w_h)^\top$ and depending on a penalty parameter $\sigma_{F,h} > 0$ and $\Theta \in \{1, -1, 0\}$ corresponding to the symmetric, asymmetric and incomplete interior penalty methods, respectively. Note that in ρ_h^Θ we only sum over boundary faces, when Dirichlet boundary conditions are applied.

To ensure a stable scheme, the penalty parameter $\sigma_{F,h} := \frac{C_\sigma}{h_F}$ must be chosen sufficiently large, see, e.g., [11, Corollary 2.41] for lower bounds on $C_\sigma > 0$. Additionally, C_σ should be selected based on the local spacial polynomial degree near F . For further details, we refer to [11, Section 7] and the references therein.

For the nonlinear terms, we consider only volume elements, so that

$$n_h(u_h, z_h) := (N(u_h, u_h), z_h)_{Q_h} = \frac{1}{2} n'_h(u_h, z_h; u_h)$$

is chosen to discretize the nonlinear terms. For the linearized equation (5), we obtain

$$n'_h(u_h, z_h; \tilde{u}_h) := (N(u_h, \tilde{u}_h) + N(\tilde{u}_h, u_h), z_h)_{Q_h}$$

with $\tilde{u}_h \in Z_h$. We remark that $n'_h(\cdot, \cdot; \tilde{u}_h)$ is the Fréchet derivative of $n_h(\cdot, \cdot)$ at \tilde{u}_h .

The complete schemes

The complete nonlinear discrete variational problem approximating equation (2) is then given by

$$\text{solve for } u_h \in Z_h \text{ such that } b_h(u_h, z_h) = \ell_h(z_h) \text{ for all } z_h \in Z_h \quad (13)$$

with

$$b_h(u_h, z_h) := m_h(u_h, z_h) + a_h(u_h, z_h) + d_h(u_h, z_h) + n_h(u_h, z_h)$$

and

$$\ell_h(z_h) := (f_h, z_h)_{Q_h} + (Mu_{0,h}, z_h(0))_{\Omega_h} + \int_0^T \ell_{\partial\Omega,h}(z_h) dt. \quad (14)$$

Depending on the boundary conditions, we have

$$\begin{aligned} \ell_{\partial\Omega,h}(z_h) := & \sum_{F \in \mathcal{F}_h^D} - (A_{\mathbf{n}}^{\text{up}} u_{D,h}, z_h)_F - \Theta(Du_{D,h}, \nabla z_h \mathbf{n}_F)_F + \sigma_{F,h}(Du_{D,h}, z_h)_F \\ & + \sum_{F \in \mathcal{F}_h^N} -(2A_{\mathbf{n}}^{\text{up}}(0, v_{N,h})^\top, z_h)_F - \Theta(D(0, v_{N,h})^\top, \nabla z_h \mathbf{n}_F)_F \\ & + \sigma_{F,h}(D(0, v_{N,h})^\top, z_h)_F + ((p_{N,h}, 0)^\top, z_h)_F, \end{aligned} \quad (15)$$

where $f_h, u_{0,h}, u_{D,h}, u_{N,h} \in Z_h$ denote suitably interpolated data. Note that the added terms in (15) ensure consistency, see Lemma 3.2. The complete linear variational problem discretizing equation (5) is given by

$$\text{solve for } u_h \in Z_h \text{ such that } b'_h(u_h, z_h; \tilde{u}_h) = \ell_h(z_h) \text{ for all } z_h \in Z_h \quad (16)$$

with $b'_h(u_h, z_h; \tilde{u}_h) = m_h(u_h, z_h) + a_h(u_h, z_h) + d_h(u_h, z_h) + n'_h(u_h, z_h; \tilde{u}_h)$.

To solve the nonlinear problem (13), we apply a Newton-Raphson method, see [9], described in Algorithm 2.1, solving the linear problem (16) in each iteration. To this end, we define the continuous residual as $r(u) := G(u)$ using (4), and the discrete residual as

$$r_h(u_h) := b_h(u_h, \cdot) - \ell_h.$$

Fixing a tolerance constant $c_{\text{tol}} > 0$ and an initial guess $u_h^{(0)}$, the following algorithm generates a sequence $u_h^{(n)} \in Z_h$, $n \in \mathbb{N}$.

Algorithm 2.1 (Newton's method). Set $r_h^{(0)} = r_h(u_h^{(0)})$ and set $n = 0$.

While $\|r_h^{(n)}\|_{L^2(Q)} > c_{\text{tol}}$ do:

1. Solve for $u_h \in Z_h$ such that $b_h(u_h, z_h; u_h^{(n)}) = r_h^{(n)}(z_h) \forall z_h \in Z_h$.
2. Update $u_h^{(n+1)} = u_h^{(n)} - u_h$, $r_h^{(n+1)} = r_h(u_h^{(n+1)})$, $n \rightarrow n + 1$.

3 Linearized system

In this section, we treat the well-posedness and convergence analysis of the linear discrete problem (16) under the condition that \tilde{u}_h is sufficiently small with respect to a suitable norm.

3.1 Preliminaries

We assume that $\sigma_{F,h}$ is chosen sufficiently large such that

$$d_h(z_h, z_h) \geq c_\Theta \int_0^T \|z_h(t)\|_h^2 dt \quad \forall z_h \in Z_h, \quad (17)$$

where $c_\Theta > 0$ is independent of h and $\|\cdot\|_h$ is defined below in (19). We refer to, e.g., [11, Corollary 2.41] for a proof of (17) and possible choices of the penalty parameter $\sigma_{F,h}$ in (12).

The analysis is carried out with respect to the h -dependent norm

$$\|u_h\|_{Z_h} := \left(\frac{1}{2} \sum_{j=0}^k \|M^{\frac{1}{2}}[u_h]_j\|_{L^2(\Omega_h)}^2 + \int_0^T c_A \|A_{\mathbf{n}}[u_h]\|_{L^2(\partial\Omega_h)}^2 + c_\Theta \|u_h\|_h^2 dt \right)^{\frac{1}{2}} \quad \text{in } Q, \quad (18)$$

where with $u_h(t) = u_h = (p_h, v_h)^\top$ for fixed t

$$\|u_h\|_h := \left(\|D^{\frac{1}{2}}\nabla u_h\|_{L^2(\Omega_h)}^2 + \beta \sum_{F \in \mathcal{F}_h \setminus \mathcal{F}_h^N} \sigma_{F,h} \| [p_h]_F \|_{L^2(F)}^2 + \zeta \sum_{F \in \mathcal{F}_h} \sigma_{F,h} \| [v_h]_F \|_{L^2(F)}^2 \right)^{\frac{1}{2}} \quad \text{in } \Omega \quad (19)$$

denotes the natural norm used for interior penalty methods. Note that in (19), as in the previous section, ∇ is understood as acting piece wise in each cell, when applied to discontinuous functions. For better readability, we sometimes write $\|u_h\|_{\star,h} := \left(\int_0^T \|u_h\|_h^2 dt \right)^{\frac{1}{2}}$.

As corresponding broken Sobolev space, we consider

$$H^1(\mathcal{K}_h) := \{w \in L^2(\Omega_h; \mathbb{R}^{1+d}) : w_K \in H^1(K; \mathbb{R}^{1+d}) \ \forall K \in \mathcal{K}_h\}$$

and equip it with the norm $\|\cdot\|_h$. In the analysis, we use the broken Poincaré inequality

$$\|u_h\|_{L^2(\Omega_h)} \leq c_P \|u_h\|_h \quad \forall u_h \in H^1(\mathcal{K}_h), \quad (20)$$

where $c_P > 0$ is independent of h , cf. [5]. Moreover, we rely on the broken Sobolev inequality

$$\|u_h\|_{L^4(\Omega_h)} \leq c_S \|u_h\|_h \quad \forall u_h \in H^1(\mathcal{K}_h), \quad (21)$$

where $c_S > 0$ is independent of h . This inequality is, as the broken Poincaré inequality, just a special case of more general broken Sobolev inequalities. For a proof of these and other generalized results, we refer the reader to [28, Theorem 3.7]. For inequalities (20), (21) to hold, we rely on the assumption that \mathcal{F}_h^D has positive $(d-1)$ -dimensional Lebesgue measure, the assumed mesh regularity, as well as $d \in \{2, 3\}$.

A key ingredient in the analysis is the following lemma.

Lemma 3.1. $\|\cdot\|_{Z_h}$ is a norm on Z_h .

Proof. $\|\cdot\|_{Z_h}$ is a semi norm, since it is defined by adding different L^2 -norms together. To show positive definiteness, let $z_h \in Z_h$ be such that $\|z_h\|_{Z_h} = 0$. In particular, this implies $\|z_h\|_h = 0$, which leads to $z_h = 0$, see [11, Section 6] for details. \square

3.2 Consistency

For a consistency result, we define a right hand side with non discrete data, cf. (14), (15), as

$$\begin{aligned} \ell(z_h) := & (f, z_h)_{Q_h} + (Mu_0, z_h(0, \cdot))_{\Omega_h} \\ & + \int_0^T \left(- (A_{\mathbf{n}}^{\text{up}} u_D, z_h)_{\Gamma_D} - \Theta(Du_D, \nabla z_h \mathbf{n})_{\Gamma_D} + \sum_{F \in \mathcal{F}_h^D} \sigma_{F,h}(Du_D, z_h)_F + ((p_N, 0)^\top, z_h)_{\Gamma_N} \right. \\ & \left. - 2(A_{\mathbf{n}}^{\text{up}}(0, v_N)^\top, z_h)_{\Gamma_N} - \Theta(D(0, v_N)^\top, \nabla z_h \mathbf{n})_{\Gamma_N} + \sum_{F \in \mathcal{F}_h^N} \sigma_{F,h}(D(0, v_N)^\top, z_h)_F \right) dt. \end{aligned}$$

Lemma 3.2. *Let $\hat{u} \in U$ be the solution to the nonlinear equation (2), and let $u \in U$ denote the solution to the linearized equation (5) with given $\tilde{u} \in U$. Then, it holds*

$$b_h(\hat{u}, z_h) = \ell(z_h) \quad \forall z_h \in Z_h \quad (22)$$

and for any $\tilde{u}_h \in Z_h$

$$b'_h(u, z_h; \tilde{u}_h) = \ell(z_h) + n'_h(u, z_h; \tilde{u}_h - \tilde{u}) \quad \forall z_h \in Z_h. \quad (23)$$

Proof. Due to the regularity of $\hat{u} \in U$, all jump terms in (16) involving interior faces vanish. In particular, for any $z_h \in Z_h$ we have

$$\begin{aligned} m_h(\hat{u}, z_h) + a_h(\hat{u}, z_h) &= (L\hat{u}, z_h)_{Q_h} + (u_0, z_h(0, \cdot))_{\Omega_h} \\ & \quad - \int_0^T (A_{\mathbf{n}}^{\text{up}} u_D, z_h)_{\Gamma_D} + 2(A_{\mathbf{n}}^{\text{up}}(0, v_N)^\top, z_h)_{\Gamma_N} dt, \end{aligned} \quad (24)$$

and with $z_h = (q_h, w_h)^\top$, using integration by parts, we obtain

$$\begin{aligned} d_h(\hat{u}, z_h) &= \int_0^T \sum_{K \in \mathcal{K}_h} (D \nabla \hat{u}, \nabla z_h)_K + \rho_h^\Theta(\hat{u}, z_h) dt \\ &= \int_0^T \sum_{K \in \mathcal{K}_h} (-(D \Delta \hat{u}, z_h)_K + (D \nabla \hat{u} \mathbf{n}_K, z_h)_{\partial K}) + \rho_h^\Theta(\hat{u}, z_h) dt \\ &= -(D \Delta \hat{u}, z_h)_{Q_h} + \int_0^T \sum_{F \in \mathcal{F}} (D \nabla \hat{u} \mathbf{n}_F, z_h)_F + \rho_h^\Theta(\hat{u}, z_h) dt \\ &= (-D \Delta \hat{u}, z_h)_{Q_h} + \int_0^T \left(\sum_{F \in \mathcal{F}_h^D} (-\Theta(Du_{D,h}, \nabla z_h \mathbf{n}_F)_F + \sigma_{F,h}(Du_{D,h}, z_h)_F) \right. \\ & \quad \left. + (p_N, q_h)_{\Gamma_N} + \zeta \sum_{F \in \mathcal{F}_h^N} (-\Theta(v_{N,h}, \nabla w_h \mathbf{n}_F)_F + \sigma_{F,h}(v_{N,h}, w_h)_F) \right) dt, \end{aligned} \quad (25)$$

where we use that $\langle \nabla \hat{u} \rangle_F = \nabla \hat{u}$ and $[\nabla \hat{u}]_F = 0$ for all $F \in \mathcal{F}_h^{\text{int}}$, cf. [10, Section 4.2.1.1].

By testing equation (2) locally in every space-time cell with $z_h \in Z_h$, and summing over every space-time cell we obtain

$$(L\hat{u} - D \Delta \hat{u} + N(\hat{u}, \hat{u}), z_h)_{Q_h} = (f, z_h)_{Q_h}.$$

Combining the previous equation with equations (24) and (25), we arrive at (22). Analogously, testing equation (5) gives

$$(Lu - D \Delta u + N(u, \tilde{u}) + N(\tilde{u}, u), z_h)_{Q_h} = (f, z_h)_{Q_h}.$$

Since equations (24) and (25) also hold when \hat{u} is replaced by u , we obtain

$$\begin{aligned} b'_h(u, z_h; \tilde{u}_h) &= b'_h(u, z_h; \tilde{u}_h) + n'_h(u, z_h; \tilde{u}) - n'_h(u, z_h; \tilde{u}) \\ &= (m_h + a_h + d_h)(u, z_h) + n'_h(u, z_h, \tilde{u}_h) + n'_h(u, z_h; \tilde{u}) - n'_h(u, z_h; \tilde{u}) \\ &= \ell(z_h) + n'_h(u, z_h; \tilde{u}_h - \tilde{u}). \end{aligned}$$

□

3.3 Well-posedness

In this section, we establish discrete well-posedness of (16) for sufficiently small \tilde{u}_h . For the dual space of a normed space X , we write X' .

Lemma 3.3. *Let $\ell_h \in Z'_h$. There exists $\varrho > 0$ such that for all $\tilde{u}_h \in Z_h$ with*

$$\max_{t \in [0, T]} \|\tilde{u}_h(t)\|_h \leq \varrho \quad (26)$$

the variational problem (16)

$$b'_h(u_h, z_h; \tilde{u}_h) = \ell_h(z_h) \quad \forall z_h \in Z_h$$

has a unique solution $u_h \in Z_h$. Moreover, there exists $c_\varrho > 0$ independent of h such that the a priori estimate

$$\|u_h\|_{Z_h} \leq c_\varrho^{-1} \|\ell_h\|_{Z'_h} \quad (27)$$

holds.

Proof. Let $u_h \in Z_h$. We show that $b'_h(u_h, z_h; \tilde{u}_h) = 0 \quad \forall z_h \in Z_h$ implies $u_h = 0$, by proving coercivity of the bilinear form $b'_h(\cdot, \cdot; \tilde{u}_h) : Z_h \times Z_h \rightarrow \mathbb{R}$ with respect to $\|\cdot\|_{Z_h}$.

Using relation (11) and integration by parts in time we obtain, cf. [8, Eq. 30],

$$m_h(u_h, u_h) + a_h(u_h, u_h) \geq \frac{1}{2} \sum_{j=0}^k \| [u_h]_j \|_{L^2(\Omega_h)}^2 + \int_0^T c_A \| A_{\mathbf{n}}[u_h] \|_{L^2(\partial\Omega_h)}^2 dt. \quad (28)$$

To estimate the trilinear form $n'_h(\cdot, \cdot; \cdot)$, we combine Hölder's inequality with the broken Sobolev inequality (21) to obtain

$$\begin{aligned} |n'_h(u_h, u_h; \tilde{u}_h)| &\leq \int_0^T \sum_{K \in \mathcal{K}_h} |(N(u_h, \tilde{u}_h) + N(\tilde{u}_h, u_h), u_h)_K| dt \\ &\leq \mu \int_0^T \sum_{K \in \mathcal{K}_h} \|\nabla u_h\|_{L^2(K)} \|u_h\|_{L^4(K)} \|\tilde{u}_h\|_{L^4(K)} + \|\nabla \tilde{u}_h\|_{L^2(K)} \|u_h\|_{L^4(K)}^2 dt \\ &\leq \mu \int_0^T \left(\left(\sum_{K \in \mathcal{K}_h} \|\nabla u_h\|_{L^2(K)}^2 \right)^{\frac{1}{2}} \left(\sum_{K \in \mathcal{K}_h} \|u_h\|_{L^4(K)}^4 \right)^{\frac{1}{4}} \left(\sum_{K \in \mathcal{K}_h} \|\tilde{u}_h\|_{L^4(K)}^4 \right)^{\frac{1}{4}} \right. \\ &\quad \left. + \left(\sum_{K \in \mathcal{K}_h} \|\nabla \tilde{u}_h\|_{L^2(K)}^2 \right)^{\frac{1}{2}} \left(\sum_{K \in \mathcal{K}_h} \|u_h\|_{L^4(K)}^4 \right)^{\frac{1}{2}} \right) dt \\ &\leq 2\mu c_S^2 D_{\max} \int_0^T \|u_h\|_h^2 \|\tilde{u}_h\|_h dt \\ &\leq C_n \left(\max_{[0, T]} \|\tilde{u}_h\|_h \right) \|u_h\|_{\star, h}^2 \end{aligned} \quad (29)$$

with $\mu := \max\{\gamma, \delta, \eta, \theta\} > 0$, $D_{\max} := \max\{\beta^{-\frac{1}{2}}, \zeta^{-\frac{1}{2}}\}$ and $C_n := 2\mu c_S^2 D_{\max} > 0$.

Combining estimates (17), (28), (29), choosing $\varrho \in (0, c_\Theta C_n^{-1})$, and using the smallness assumption on \tilde{u}_h (26) gives

$$\begin{aligned} b'_h(u_h, u_h; \tilde{u}_h) &\geq m_h(u_h, u_h) + a_h(u_h, u_h) + d_h(u_h, u_h) - |n'_h(u_h, u_h; \tilde{u}_h)| \\ &\geq \frac{1}{2} \sum_{j=0}^k \| [u_h]_j \|_{L^2(\Omega_h)}^2 + \int_0^T c_A \| A_{\mathbf{n}}[u_h] \|_{L^2(\partial\Omega_h)}^2 + (c_\Theta - \varrho C_n) \| u_h \|_h^2 \, dt \\ &\geq c_\varrho \| u_h \|_{Z_h}^2 \end{aligned} \quad (30)$$

with $c_\varrho := \min\{1, c_\Theta - \varrho C_n\}$ independent of h . This shows coercivity and the a priori estimate (27) follows by means of standard methods, see e.g. [10, Lemma 1.4]. \square

3.4 Convergence in the discontinuous Galerkin norm

In this section, we establish convergence of the linear DG scheme (16) with respect to $\| \cdot \|_{Z_h}$. To this end, we first introduce relevant projections. Let $\Pi_h : L^2(\Omega; \mathbb{R}^i) \rightarrow \mathcal{P}_h(\Omega; \mathbb{R}^i)$ with $i \in \mathbb{N}$ denote the spatial L^2 -projection defined by

$$(\Pi_h u, z_h)_\Omega = (u, z_h)_\Omega \quad \forall z_h \in \mathcal{P}_h(\Omega; \mathbb{R}^i)$$

and $\pi_h : C(0, T; L^2(\Omega; \mathbb{R}^{1+d})) \rightarrow Z_h$ denote the space-time projection with the following properties

- (i) $\pi_h u \in Z_h$,
- (ii) $(\pi_h u)_j(x, t_j) = \Pi_h u_j(x, t_j)$ for a.e. $x \in \Omega$ and $j \in \{1, \dots, k\}$ with $i = 1 + d$,
- (iii) $\int_{I_j} (\pi_h u - u, z_h)_\Omega \, dt = 0 \quad \forall z_h \in Z_h^-$ and $j \in \{1, \dots, k\}$,

cf. [11, Section 6.1.4], where existence and uniqueness among other properties of π_h are shown. We denote by Z_h^- the space obtained when decreasing the polynomial time degrees by one in each space-time cell. Due to this property, we assume for the rest of the paper that, the time degrees of each cell are at least one. The following result is the basis for an estimate of the numerical error in terms of projection errors.

Lemma 3.4. *Let $u \in U$ be the solution to the continuous linear system (5) with $\tilde{u} \in U$ and $u_h \in Z_h$ the solution to the discrete linear problem (16) with $\tilde{u}_h \in Z_h$ such that (26) holds with $\varrho > 0$ as in Lemma 3.3. Then*

$$\begin{aligned} \|u_h - \pi_h u\|_{Z_h}^2 &\leq C_Z \left(\sum_{j=1}^k \|M^{\frac{1}{2}}(\pi_h u - u)_j(t_j)\|_{L^2(\Omega_h)}^2 + \int_0^T \left(\|\pi_h u - u\|_{L^2(\partial\Omega_h)}^2 + \|\pi_h u - u\|_h^2 \right) \, dt \right) \\ &\quad + C_R \left(\|\ell_h - \ell\|_{Z_h'}^2 + \|\tilde{u}_h - \tilde{u}\|_{\star, h}^2 \right) \end{aligned}$$

with $C_Z, C_R > 0$ independent of h .

Proof. By consistency, see Lemma 3.2 equation (23), it holds for all $z_h \in Z_h$

$$b'_h(u_h - u, z_h; \tilde{u}_h) = b'_h(u_h, z_h; \tilde{u}_h) - b'_h(u, z_h; \tilde{u}_h) = \ell_h(z_h) - \ell(z_h) - n'_h(u, z_h; \tilde{u}_h - \tilde{u}),$$

which is equivalent to

$$b'_h(u_h - \pi_h u, z_h; \tilde{u}_h) = -b'_h(\pi_h u - u, z_h; \tilde{u}_h) + \ell_h(z_h) - \ell(z_h) - n'_h(u, z_h; \tilde{u}_h - \tilde{u}).$$

Choosing $z_h = u_h - \pi_h u \in Z_h$, defining remainder terms $\mathcal{C}_h := |(\ell_h - \ell)(u_h - \pi_h u)| + |n'_h(u, u_h - \pi_h u; \tilde{u}_h - \tilde{u})|$, and by coercivity of b'_h derived in the proof of Lemma 3.3, see equation (30), we obtain

$$c_\varrho \|u_h - \pi_h u\|_{Z_h}^2 \leq |b'_h(\pi_h u - u, u_h - \pi_h u; \tilde{u}_h)| + \mathcal{C}_h. \quad (31)$$

For the rest of the proof, we estimate the right hand side of (31) further. Starting with m_h , we have for all $z_h \in Z_h$ using partial integration in time, property (iii) of π_h , Hölder's inequality, and Young's inequality

$$\begin{aligned} |m_h(\pi_h u - u, z_h)| &= \left| \sum_{j=1}^k \int_{t_{j-1}}^{t_j} (M \partial_t(\pi_h u - u), z_h)_{\Omega_h} dt + (M[\pi_h u - u]_{j-1}, z_{h,j}(t_{j-1}))_{\Omega_h} \right| \\ &= \left| \sum_{j=1}^k - \int_{t_{j-1}}^{t_j} (M(\pi_h u - u), \partial_t z_h)_{\Omega_h} dt - (M(\pi_h u - u)_j(t_j), [z_h]_j)_{\Omega_h} \right| \\ &= \left| \sum_{j=1}^k (M^{\frac{1}{2}}(\pi_h u - u)_j(t_j), M^{\frac{1}{2}}[z_h]_j)_{\Omega_h} \right| \\ &\leq \sqrt{2} \left(\sum_{j=1}^k \|M^{\frac{1}{2}}(\pi_h u - u)_j(t_j)\|_{L^2(\Omega_h)}^2 \right)^{\frac{1}{2}} \left(\frac{1}{2} \sum_{j=1}^k \|M^{\frac{1}{2}}[z_h]_j\|_{L^2(\Omega_h)}^2 \right)^{\frac{1}{2}} \\ &\leq \frac{2\sqrt{2}}{c_\varrho} \sum_{j=1}^k \|M^{\frac{1}{2}}(\pi_h u - u)_j(t_j)\|_{L^2(\Omega_h)}^2 + \frac{c_\varrho}{8} \|z_h\|_{Z_h}^2, \end{aligned}$$

cf. [11, Section 6.1]. For a_h , we have for all $z_h \in Z_h$ using Hölder's inequality, Lemma A.2, discrete Poincaré inequality (20), and relation (11)

$$\begin{aligned} |a_h(\pi_h u - u, z_h)| &\leq \int_0^T \sum_{K \in \mathcal{K}_h} \left(\|A(\pi_h u - u)\|_{L^2(K)} \|z_h\|_{L^2(K)} + \sum_{F \in \mathcal{F}_K} \|\pi_h u - u\|_{L^2(F)} \|A_{\mathbf{n}_K}^{\text{up}}[z_h]_{F,K}\|_{L^2(F)} \right) dt \\ &\leq \int_0^T \|\nabla(\pi_h u - u)\|_{L^2(\Omega_h)} \|z_h\|_{L^2(\Omega_h)} + 2C_A \|\pi_h u - u\|_{L^2(\partial\Omega_h)} \|A_{\mathbf{n}}[z_h]\|_{L^2(\partial\Omega_h)} dt \\ &\leq \int_0^T \frac{2c_P D_{\max}}{c_\varrho c_\Theta} \|\pi_h u - u\|_h^2 + \frac{c_\varrho c_\Theta}{8} \|z_h\|_h^2 + \frac{4C_A}{c_\varrho c_A} \|\pi_h u - u\|_{L^2(\partial\Omega_h)}^2 dt + \frac{c_\varrho}{8} \|z_h\|_{Z_h}^2. \end{aligned}$$

For d_h , we have for all $z_h \in Z_h$ using Hölder's inequality and Young's inequality

$$\begin{aligned} |d_h(\pi_h u - u, z_h)| &\leq \int_0^T \|D^{\frac{1}{2}} \nabla(\pi_h u - u)\|_{L^2(\Omega_h)} \|D^{\frac{1}{2}} \nabla z_h\|_{L^2(\Omega_h)} + |\rho_h^\Theta(\pi_h u - u, z_h)| dt \\ &\leq \int_0^T \|\pi_h u - u\|_h \|z_h\|_h + |\rho_h^\Theta(\pi_h u - u, z_h)| dt \\ &\leq \int_0^T \frac{2}{c_\varrho c_\Theta} \|\pi_h u - u\|_h^2 + \frac{c_\varrho c_\Theta}{8} \|z_h\|_h^2 + |\rho_h^\Theta(\pi_h u - u, z_h)| dt, \end{aligned}$$

while for $C_{\text{ip}} > 0$ independent of h

$$|\rho_h^\Theta(\pi_h u - u, z_h)| \leq C_{\text{ip}} D_{\max}^2 \|\pi_h u - u\|_h \|z_h\|_h \leq \frac{2C_{\text{ip}} D_{\max}^2}{c_\varrho c_\Theta} \|\pi_h u - u\|_h^2 + \frac{c_\varrho c_\Theta}{8} \|z_h\|_h^2,$$

which can be proven by combining [10, Lemma 4.16] and [10, Lemma 4.20]. Finally, for n'_h , we have for all $z_h \in Z_h$ using estimates as in (29), $\max_{[0,T]} \|\tilde{u}_h\|_h \leq \varrho$, and Young's inequality

$$|n'_h(\pi_h u - u, z_h; \tilde{u}_h)| \leq \int_0^T \frac{2C_n \varrho}{c_\varrho c_\Theta} \|\pi_h u - u\|_h^2 + \frac{c_\varrho c_\Theta}{8} \|z_h\|_h^2 dt.$$

Choosing $z_h = u_h - \pi_h u \in Z_h$, and absorbing the $\|\cdot\|_{Z_h}$ terms into the left hand side of (31), we obtain

$$\frac{c_\varrho}{4} \|u_h - \pi_h u\|_{Z_h}^2 \leq C_b \left(\sum_{j=1}^k \|M^{\frac{1}{2}}(\pi_h u - u)_j(t_j)\|_{L^2(\Omega_h)}^2 + \int_0^T \|\pi_h u - u\|_{L^2(\partial\Omega_h)}^2 + \|\pi_h u - u\|_h^2 dt \right) + C_h$$

with $C_b := 2c_\varrho^{-1} \max\{\sqrt{2}, \frac{c_P D_{\max}}{c_\Theta}, \frac{2C_A}{c_A}, \frac{1}{c_\Theta}, \frac{C_{\text{ip}} D_{\max}^2}{c_\Theta}, \frac{C_n \varrho}{c_\Theta}\} > 0$. Since

$$C_h \leq \frac{c_\varrho}{16} \|\pi_h u - u\|_{Z_h}^2 + \frac{4}{c_\varrho} \|\ell_h - \ell\|_{Z'_h}^2 + \frac{c_\varrho}{16} \|u_h - \pi_h u\|_{Z_h}^2 + \frac{4C_n c_\Theta \max_{[0,T]} \|u\|_h}{c_\varrho} \|\tilde{u}_h - \tilde{u}\|_{\star,h}^2,$$

using Young's inequality and (29), we obtain the result with $C_R := \frac{32}{c_\varrho^2} \max\{1, C_n c_\Theta \max_{[0,T]} \|u\|_h\}$ and $C_Z := \frac{8C_b}{c_\varrho}$. \square

Remark 3.1. For matters of readability, we use $\|\cdot\|_h$ to estimate $\|\nabla(\pi_h u - u)\|_{L^2}$ and $\|\pi_h u - u\|_{L^4}$. In principle, one does not have to do this and one would obtain slightly better constants $C_P, C_{p'}$ in the resulting error estimate cf. Theorem 3.1. However, the overall scaling with h in the error estimate is not affected.

Remark 3.2. Note that $\max_{t \in [0,T]} \|u(t)\|_h$ is uniformly bounded in h for $u \in U$. This follows from the Sobolev embedding $L^\infty(0, T; H^1(\Omega)) \hookrightarrow L^2(0, T; H^2(\Omega)) \cap H^1(0, T; L^2(\Omega))$, see [15, Sect. 5.9, Thm. 4] and the fact that $\|u\|_h \leq C_U \|u\|_{H^1(\Omega)}$ for some $C_U > 0$ independent of h .

To complete the convergence analysis, we estimate the projection errors of π_h in terms of h . For this, we define the following semi-norms

$$\begin{aligned} |u|_{H^s(\Omega)} &= \left(\int_{\Omega} \sum_s |\partial_x^s u|^2 dx \right)^{\frac{1}{2}}, \\ |u|_{H^p(0,T;H^s(\Omega))} &= \left(\int_0^T |\partial_t^p u|_{H^s(\Omega)}^2 dt \right)^{\frac{1}{2}}, \\ |u|_{C(0,T;H^s(\Omega))} &= \max_{[0,T]} |u|_{H^s(\Omega)}, \\ \|u\|_{H^p(0,T;H^1(\Omega))} &= \left(|u|_{H^p(0,T;L^2(\Omega))}^2 + |u|_{H^p(0,T;H^1(\Omega))}^2 \right)^{\frac{1}{2}}, \end{aligned}$$

where ∂_x^s stands for spatial partial derivatives of order $s \in \mathbb{N}$. The next lemma mainly uses results from [11, Section 6]. In the following, we set $\vartheta = 1$ if for the Dirichlet data with global minimal time degree p we have

$$u_D(x, t) = \sum_{j=0}^p \Psi_j(x) t^j \tag{32}$$

with $\Psi_j \in H^{s-\frac{1}{2}}(\Gamma_D; \mathbb{R}^{1+d})$, $s \geq 1$ and $\vartheta = 0$ otherwise.

Lemma 3.5. *Let*

$$V := H^{p+1}(0, T; H^1(\Omega; \mathbb{R}^{1+d})) \cap W^{p+1, \infty}(0, T; L^2(\Omega; \mathbb{R}^{1+d})) \cap C([0, T]; H^s(\Omega; \mathbb{R}^{1+d})) \quad (33)$$

with $p = \min_{R \in \mathcal{R}_h} p_R$ the global minimal time degree, $q = \min_{R \in \mathcal{R}_h} q_R$ the global minimal space degree, $\nu = \min\{q+1, s\}$ with $s \geq 1$, $\omega \in [1, \infty)$ the constant from (6) and $\vartheta \in \{0, 1\}$ the constant determined by (32). Then, the following projection error estimates hold for $u \in V$

$$\sum_{j=0}^k \|M^{\frac{1}{2}}[\pi_h u - u]_j\|_{L^2(\Omega_h)}^2 \leq C_1 \left(h^{2\nu-\omega} |u|_{C(0,T;H^\nu(\Omega))}^2 + h^{2(p+1)-\omega} |u|_{W^{p+1,\infty}(0,T;L^2(\Omega))}^2 \right), \quad (34)$$

$$\sum_{j=1}^k \|M^{\frac{1}{2}}(\pi_h u - u)_j(t_j)\|_{L^2(\Omega_h)}^2 \leq C_2 h^{2\nu-\omega} |u|_{C(0,T;H^\nu(\Omega))}^2, \quad (35)$$

$$\int_0^T \| \pi_h u - u \|_h^2 dt \leq C_3 \left(h^{2(\nu-1)} |u|_{C(0,T;H^\nu(\Omega))}^2 + h^{2(p+\vartheta)} |u|_{H^{p+1}(0,T;H^1(\Omega))}^2 \right), \quad (36)$$

$$\int_0^T \| \pi_h u - u \|_{L^2(\partial\Omega_h)}^2 dt \leq C_4 \left(h^{2(\nu-\frac{1}{2})} |u|_{C(0,T;H^\nu(\Omega))}^2 + h^{2(p+\frac{1}{2})} |u|_{H^{p+1}(0,T;L^2(\Omega))}^2 \right), \quad (37)$$

$$\int_0^T c_A \|A_{\mathbf{n}}[\pi_h u - u]\|_{L^2(\partial\Omega_h)}^2 dt \leq C_5 \left(h^{2(\nu-\frac{1}{2})} |u|_{C(0,T;H^\nu(\Omega))}^2 + h^{2(p+\frac{1}{2})} |u|_{H^{p+1}(0,T;L^2(\Omega))}^2 \right), \quad (38)$$

where C_1 to C_5 are positive constants independent of h .

Proof. From [11, Lemma 6.22, Eq. (6.136)] we get, using (6) and taking $\sup_{[0,T]}$,

$$\| \pi_h u - u \|_{C(0,T;L^2(\Omega_h))}^2 \leq 2C_\pi^2 \left(h^{2\nu} |u|_{C(0,T;H^\nu(\Omega))}^2 + c_r^{-2(p+1)} h^{2(p+1)} |u|_{W^{p+1,\infty}(0,T;L^2(\Omega))}^2 \right) \quad (39)$$

with $C_\pi > 0$ independent of h . To derive projection error estimate (34), we use relation (6) together with $(k+1) \leq C_s \tau^{-1}$ with $C_s > 0$, which holds due to shape regularity, so that

$$\sum_{j=0}^k \|[\pi_h u - u]_j\|_{L^2(\Omega_h)}^2 \leq 2(k+1) \| \pi_h u - u \|_{C(0,T;L^2(\Omega))}^2 \leq 2C_s c_r h^{-\omega} \| \pi_h u - u \|_{C(0,T;L^2(\Omega))}^2.$$

Combining this with (39), we obtain (34) with $C_1 = 4C_s c_r C_\pi^2 \max\{1, c_r^{-2(p+1)}\} \max\{\alpha^{-\frac{1}{2}}, \varepsilon^{-\frac{1}{2}}\}$.

According to [11, Lemma 6.17, Eq. 107], we have for $j = 1, \dots, k$

$$\|(\pi_h u - u)_j(t_j)\|_{L^2(\Omega_h)}^2 \leq C_l h^{2\nu} |u_j(t_j)|_{H^\nu(\Omega)}^2$$

with $C_l > 0$ independent of h . Summing over j , taking supremum over j , using $k \leq C_s \tau^{-1}$, and mesh balance (6) gives (35) with $C_2 = C_l C_s c_r$.

Due to [11, Lemma 6.22, Eq. 134], we have for $j = 1, \dots, k$

$$\int_{I_j} \|u - \pi_h u\|_h^2 dt \leq C_{\|} \left(h^{2(\nu-1)} |u|_{L^2(I_j;H^\nu(\Omega))}^2 + \tau_j^{2(p+\vartheta)} |u|_{H^{p+1}(I_j;H^1(\Omega))}^2 \right)$$

with $C_{\|} > 0$ independent of h . From there, equation (36) follows by summing over j , using (6) $c_r \tau \leq h$, and $|u|_{L^2(0,T;H^\nu(\Omega))}^2 \leq T |u|_{C(0,T;H^\nu(\Omega))}^2$ with $C_3 = C_{\|} T \max\{1, c_r^{-2(p+\vartheta)}\}$.

By the discrete trace inequality, cf. [10, Remark 1.47], we have

$$\| \pi_h u - u \|_{L^2(\partial\Omega_h)}^2 \leq \sum_{K \in \mathcal{K}_h} \|u - \pi_h u\|_{L^2(\partial K)}^2 \leq C_{\text{tr}} h^{-1} \sum_{K \in \mathcal{K}_h} \|u - \pi_h u\|_{L^2(K)}^2$$

with $C_{\text{tr}} > 0$ independent of h . Combining this with relation (39) gives

$$\int_0^T \|u - \pi_h u\|_{L^2(\partial\Omega)}^2 dt \leq 2h^{-1} C_{\text{tr}} C_\pi^2 \left(h^{2\nu} |u|_{C(0,T;H^\nu)}^2 + h^{2(p+1)} |u|_{W^{p+1,\infty}(0,T;L^2(\Omega))}^2 \right),$$

which yields equation (37) with $C_4 = 2C_{\text{tr}} C_\pi^2 \max\{1, c_r^{-2(p+1)}\}$.

Similarly, equation (38) with $C_5 = 2C_4$ can be obtained, since

$$\|A_{\mathbf{n}}[\pi_h u - u]\|_{L^2(\partial\Omega_h)}^2 \leq 2\|\pi_h u - u\|_{L^2(\partial\Omega)}^2.$$

□

The following theorem provides a complete error estimate for the linearized system in terms of h .

Theorem 3.1. *Let $u \in V$ with V from (33) be a solution to the continuous linear system (5) with $\tilde{u} \in U$ and let $u_h \in Z_h$ be a solution to the discrete linear system (16) with $\tilde{u}_h \in Z_h$ such that (26) holds with $\varrho > 0$ as in Lemma 3.3.*

Furthermore, let $p = \min_{R \in \mathcal{R}_h} p_R$ be the global minimal time degree, $q = \min_{R \in \mathcal{R}_h} q_R$ be the global minimal space degree, $\omega \in [1, \infty)$ the constant from (6), $\vartheta \in \{0, 1\}$ the constant determined by (32), and $\xi = \min\{p + \vartheta, p + 1 - \frac{\omega}{2}, \nu - \frac{\omega}{2}, \nu - 1\}$ with $\nu = \min\{q + 1, s\}$, $s \geq 2$. Then

$$\|u_h - u\|_{Z_h} \leq C_P h^\xi + C_Q (\|\ell_h - \ell\|_{Z'_h} + \|\tilde{u}_h - \tilde{u}\|_{\star,h})$$

with $C_P, C_Q > 0$ independent of h .

Proof. By the triangle inequality, we have

$$\|u_h - u\|_{Z_h} \leq \|u_h - \pi_h u\|_{Z_h} + \|\pi_h u - u\|_{Z_h}.$$

From Lemma 3.5 we obtain, when taking square roots,

$$\|\pi_h u - u\|_{Z_h} \leq C_6 h^\xi$$

using the projection estimates (34), (36), (38). Combining Lemma 3.4 with the projection estimates (35), (36), (37) from Lemma 3.5 we obtain, when taking square roots,

$$\|\pi_h u - u_h\|_{Z_h} \leq C_7 h^\xi + C_8 (\|\ell_h - \ell\|_{Z'_h} + \|\tilde{u}_h - \tilde{u}\|_{\star,h}),$$

yielding the error estimate for the linear problem, since the constants $C_6, C_7, C_8 > 0$ are only depending on $\|u\|_V, C_Z, C_R$ and C_i with $i = 1, \dots, 5$. □

Remark 3.3. *We note that $U \subset V$ for $p = 0$. If $\vartheta = \omega = 1$, Theorem 3.1 yields convergence in h if*

$$u \in H^1(0, T; H^1(\Omega; \mathbb{R}^{1+d})) \cap W^{1,\infty}(0, T; L^2(\Omega; \mathbb{R}^{1+d})) \cap C(0, T; H^2(\Omega; \mathbb{R}^{1+d}))$$

choosing $p = 0$, $q = 1$ and $s = 2$. A convergence analysis for less regular solutions is not contained in this paper.

4 Nonlinear system

We are now in a position to apply a general existence and convergence result for Newton's method to the nonlinear discrete problem (13), namely, a generalized Newton-Kantorovich Theorem, see [21, Theorem 2.1]. We restate the theorem for the reader's convenience.

Lemma 4.1. *Let X and Y be Banach spaces and $G : \mathcal{D}(G) \subseteq X \rightarrow Y$. Suppose that on an open convex set $D_* \subseteq \mathcal{D}(G)$, G is Fréchet differentiable and G' is χ -Hölder continuous in D_* with exponent $\chi \in (0, 1]$ and constant $\lambda > 0$, i.e.,*

$$\|G'_{u_1} - G'_{u_2}\|_{\mathcal{L}(X,Y)} \leq \lambda \|u_1 - u_2\|_X^\chi, \quad u_1, u_2 \in D_*.$$

For some $u_* \in D_*$, assume $\Gamma_* := (G'_{u_*})^{-1}$ is defined on all of Y and

$$v = \kappa \lambda \phi^\chi \leq \chi_0 \quad \text{with } \kappa = \|\Gamma_*\|_{\mathcal{L}(Y,X)}, \quad \phi = \|\Gamma_* G(u_*)\|_X, \quad (40)$$

where $\chi_0 \in (0, \frac{1}{2}]$ is the unique root of $w \mapsto (1 + \chi)^\chi (1 - w)^{1+\chi} - w^\chi$. Set

$$\varrho = \frac{\phi(1 + \chi)(1 - v)}{(1 + \chi) - (2 + \chi)v}, \quad \tilde{\varrho} = \phi v^{-\frac{1}{\chi}} \quad (41)$$

and suppose that $B_\varrho^X(u_*) \subseteq D_*$. Then, the Newton iterates

$$u^{(n+1)} = u^{(n)} - G_{u^{(n)}}'^{-1} G(u^{(n)}), \quad n = 0, 1, 2, \dots$$

starting at $u^{(0)} := u_*$ are well-defined, lie in $B_\varrho^X(u_*)$ and converge to a solution of $G(u) = 0$, which is unique in $B_{\tilde{\varrho}}^X(u_*) \cap D_*$. Moreover, if strict inequality holds in (40), the order of convergence is at least $1 + \chi$.

Building upon the results of the previous section, we derive the following local well-posedness and convergence result for the nonlinear problem (13). In the proof, we use that $\|u\|_{Z_h} \leq C_U \|u\|_U$ for $u \in U$ and some $C_U > 0$ independent of h cf. Remark 3.2.

Theorem 4.1. *Let $u \in V$ with V from (33) be a solution to the continuous nonlinear system (2) and assume that*

$$\|u\|_U \leq \varrho_U, \quad \|\ell_h\|_{Z'_h} \leq \varrho_\ell, \quad (42)$$

where $\varrho_U > 0$ and $\varrho_\ell > 0$ are assumed to be sufficiently small.

Furthermore, let $p = \min_{R \in \mathcal{R}_h} p_R$ be the minimal global time degree, $q = \min_{R \in \mathcal{R}_h} q_R$ be the minimal global space degree, $\omega \in [1, \infty)$ the constant from (6), $\vartheta \in \{0, 1\}$ the constant determined by (32), $\xi = \min\{p + \vartheta, p + 1 - \frac{\omega}{2}, \nu - \frac{\omega}{2}, \nu - 1\}$ with $\nu = \min\{q + 1, s\}$, $s \geq 2$, and $\chi \in (0, 1]$ such that $(1 - \chi) \min\{p + \vartheta, p + 1 - \frac{\omega}{2}\} \geq \frac{\omega}{2}$. We also assume that $\min\{p + \vartheta - \omega, p + 1 - \frac{3\omega}{2}\} > 0$ and $\nu > \omega$. For $\bar{h} > 0$ define

$$D_{\bar{h},*} := \{u_h \in Z_h : (\bar{h}^{-\min\{p+\vartheta, p+1-\frac{\omega}{2}\}} + \bar{h}^{-\min\{\nu-\frac{\omega}{2}, \nu-1\}}) \|u_h - u\|_{Z_h} < C_*\}$$

with $C_* > 0$ independent of \bar{h} . Then, there exists a $\tilde{h} < \bar{h}$ such that for all $h < \tilde{h}$

$$b_h(u_h, z_h) = \ell_h(z_h) \quad \forall z_h \in Z_h$$

has a unique solution $u_h \in Z_h$ and $(1 + \chi)$ -order of convergence in Algorithm 2.1 with initial guess $u_{h,*} \in D_{h,*}$ holds. Moreover, we have the following error estimate

$$\|u_h - u\|_{Z_h} \leq C_* h^\xi.$$

Proof. Let $h \leq \bar{h} < 1$. We apply Lemma 4.1 to

$$G_h : Z_h \rightarrow Z'_h \text{ defined by } \langle G_h(u_h), \cdot \rangle_{Z'_h} = b_h(u_h, \cdot) - \ell_h(\cdot)$$

using the open, convex set $D_{\bar{h},*} \subset Z_h$. Note that due to Lemma 3.5, $D_{*,h}$ is non-empty, when choosing C_* suitably, since then $\pi_h u \in D_{*,h}$. This follows from the projection error estimates, trace inequality and inverse inequality, see equations (46), (47) below.

The Fréchet derivative of G_h at \tilde{u} evaluates to $b'_h(u_h, z_h; \tilde{u})$, cf. [22, Lemma 3.2]. First, we show its well-posedness on $D_{*,\bar{h}}$ using Lemma 3.3. For $u_{h,*}$ in $D_{h,*}$ we have

$$\begin{aligned} \max_{[0,T]} \|u_{h,*}\|_h &\leq \max_{[0,T]} \|u_{h,*} - u\|_h + \max_{[0,T]} \|u\|_h \\ &\leq C_{\text{inv}} \tau^{-\frac{1}{2}} \|u_{h,*} - u\|_{\star,h} + C_U \|u\|_U \\ &\leq C_{\text{inv}} h^{-\frac{\omega}{2}} \sqrt{c_r} c_{\Theta}^{-1} \|u_{h,*} - u\|_{Z_h} + C_U \varrho_U \\ &\leq C_{\text{inv}} \sqrt{c_r} c_{\Theta}^{-1} C_* \bar{h}^{\min\{p+\vartheta-\frac{\omega}{2}, p+1-\frac{\omega}{2}\}} + C_U \varrho_U \end{aligned} \quad (43)$$

where $C_U > 0$ from Remark 3.2 is used, $C_{\text{inv}} > 0$ comes from an inverse inequality to estimate the L^∞ -norm with respect to the L^2 -norm in time, mesh balance (6) and $\|u_{h,*} - u\|_{Z_h} < C_* h^{\min\{p+\vartheta, p+1-\frac{\omega}{2}\}}$ is used. Choosing \bar{h} and ϱ_U small enough, we obtain due to Lemma 3.3 well-posedness of the variational problem

$$b'_h(\hat{u}_h, z_h, u_{h,*}) = \hat{\ell}_h(z_h) \quad \forall z_h \in Z_h$$

with an h -independent a priori estimate $\|\hat{u}_h\|_{Z_h} \leq c_*^{-1} \|\hat{\ell}_h\|_{Z'_h}$ for all $h < \bar{h}$. If $h < \bar{h} < 1$ and if we deduce $\kappa = \frac{1}{c_*}$ from the apriori estimate, it follows that $G'_{h,u_{h,*}} : Z_h \rightarrow Z'_h$ is invertible for all $u_* \in D_{h,*}$.

To establish the Hölder estimate of G'_h , we proceed analogously to estimate (29) and combine it again with an inverse inequality to obtain for $u_1, u_2 \in D_{h,*}$ and all $u_h, z_h \in Z_h$

$$\begin{aligned} |b'_h(u_h, z_h; u_1) - \ell_h(z_h) - b'_h(u_h, z_h; u_2) + \ell_h(z_h)| &= |n'_h(u_h, z_h; u_1 - u_2)| \\ &\leq C_n c_{\Theta}^{-2} \max_{[0,T]} \|u_1 - u_2\|_h \|z_h\|_{Z_h} \|u_h\|_{Z_h} \\ &\leq C_n c_{\Theta}^{-3} C_{\text{inv}} \sqrt{c_r} 2h^{-\frac{\omega}{2}} \|u_1 - u_2\|_{Z_h} \|z_h\|_{Z_h} \|u_h\|_{Z_h} \\ &\leq C_n c_{\Theta}^{-3} C_{\text{inv}} \sqrt{c_r} 2h^{-\frac{\omega}{2}} \|u_1 - u_2\|_{Z_h}^{1-\chi} \|u_1 - u_2\|_{Z_h}^{\chi} \|z_h\|_{Z_h} \|u_h\|_{Z_h} \\ &\leq C_n c_{\Theta}^{-3} C_{\text{inv}} \sqrt{c_r} h^{-\frac{\omega}{2}} (2C_* h^{\min\{p+\vartheta, p+1-\frac{\omega}{2}\}})^{1-\chi} \|u_1 - u_2\|_{Z_h}^{\chi} \|z_h\|_{Z_h} \|u_h\|_{Z_h} \\ &\leq \lambda \|u_1 - u_2\|_{Z_h}^{\chi} \|z_h\|_{Z_h} \|u_h\|_{Z_h}, \end{aligned}$$

so that the χ -Hölder continuity holds with $\lambda \leq C_n c_{\Theta}^{-3} C_{\text{inv}} \sqrt{c_r} (2C_*)^{1-\chi}$ independent of h , due to the assumption $(1-\chi) \min\{p+\vartheta, p+1-\frac{\omega}{2}\} \geq \frac{\omega}{2}$ and $\bar{h} < 1$.

In order to fulfill assumption (40), we establish an estimate on $\|G(u_{h,*})\|_{Z'_h}$. Let $u_* \in V$ denote a function such that $\pi_h u_* = u_{h,*} \in D_{h,*}$.

Then by triangle inequality and as in the proof of Lemma 3.4

$$\begin{aligned}
|m_h(u_{h,*}, z_h)| &= \left| \sum_{j=1}^k \int_{t_{j-1}}^{t_j} (M \partial_t u_{h,*}, z_h)_{\Omega_h} dt + (M[u_{h,*}]_{j-1}, z_{h,j}(t_{j-1}))_{\Omega_h} \right| \\
&= \left| \sum_{j=1}^k - \int_{t_{j-1}}^{t_j} (M u_{h,*}, \partial_t z_h)_{\Omega_h} dt - (M(u_{h,*})_j(t_j), [z_h]_j)_{\Omega_h} \right| \\
&\leq \left| \sum_{j=1}^k - \int_{t_{j-1}}^{t_j} (M(u_{h,*} - u_*), \partial_t z_h)_{\Omega_h} dt - (M(u_{h,*})_j(t_j), [z_h]_j)_{\Omega_h} \right| + |(M \partial_t u_*, z_h)_Q| \\
&= \left| \sum_{j=1}^k (M^{\frac{1}{2}}(u_{h,*})_j(t_j), M^{\frac{1}{2}}[z_h]_j)_{\Omega_h} \right| + |(M \partial_t u_*, z_h)_Q| \\
&\leq C_M (\|u_{h,*}\|_{H^1(0,T;L^2(\Omega))} + \|\partial_t u_*\|_{L^2(0,T;L^2(\Omega))}) \|z_h\|_{Z_h},
\end{aligned}$$

where we use a trace like inequality on $(u_{h,*})_j$, so that time evaluations can be estimated by the H^1 norm. As in the proof of Lemma 3.4 we have

$$\begin{aligned}
|a_h(u_{h,*}, z_h)| &\leq \int_0^T \|\nabla u_{h,*}\|_{L^2(\Omega_h)} \|z_h\|_{L^2(\Omega_h)} + 2C_A \|u_{h,*}\|_{L^2(\partial\Omega_h)} \|A_{\mathbf{n}}[z_h]\|_{L^2(\partial\Omega_h)} dt \\
&\leq C_{\tilde{A}} (\|u_{h,*}\|_{Z_h} + \|u_{h,*}\|_{L^2(0,T;L^2(\partial\Omega_h))}) \|z_h\|_{Z_h},
\end{aligned}$$

and

$$\begin{aligned}
|d_h(u_{h,*}, z_h)| &\leq \int_0^T (\|D^{\frac{1}{2}}\nabla u_{h,*}\|_{L^2(\Omega_h)} \|D^{\frac{1}{2}}\nabla z_h\|_{L^2(\Omega_h)} + |\rho_h^\Theta(u_{h,*}, z_h)|) dt \\
&\leq \int_0^T (1 + 2C_{\text{ip}} D_{\max}^2) \|u_{h,*}\|_h \|z_h\|_h dt \\
&\leq C_D \|u_{h,*}\|_{Z_h} \|z_h\|_{Z_h},
\end{aligned}$$

as well as from estimate (43)

$$\begin{aligned}
|n_h(u_{h,*}, z_h)| &= \frac{1}{2} |n'_h(u_{h,*}, z_h; u_{h,*})| \leq \frac{1}{2} |n'_h(u_{h,*}, z_h; u_{h,*} - u)| + \frac{1}{2} |n'_h(u_{h,*}, z_h; u)| \\
&\leq C_N \|u_{h,*}\|_{Z_h} \|z_h\|_{Z_h}
\end{aligned}$$

with $C_N \leq C_n (C_{\text{inv}} \sqrt{c_r} c_\Theta^{-3} C_* + C_U \varrho_U)$. Combining the estimates, we conclude with the discrete Poincaré inequality (20) and triangle inequality

$$\begin{aligned}
\|G(u_{h,*})\|_{Z'_h} &\leq C_G (\|u_{h,*}\|_{Z_h} + \|u_{h,*}\|_{L^2(0,T;L^2(\partial\Omega_h))} \\
&\quad + \|\partial_t u_{h,*}\|_{L^2(0,T;L^2(\Omega))} + \|\partial_t(u_{h,*} - u_*)\|_{L^2(0,T;L^2(\Omega))})
\end{aligned} \tag{44}$$

with $C_G > 0$ independent of h . Note that by triangle inequality

$$\|u_{h,*}\|_{Z_h} \leq \|u_{h,*} - u\|_{Z_h} + \|u\|_{Z_h} \leq C_* \bar{h}^\xi + C_U \varrho_u, \tag{45}$$

and in combination with a discrete trace inequality

$$\begin{aligned}
\|u_{h,*}\|_{L^2(0,T;L^2(\partial\Omega_h))} &\leq C_{\text{tr}} h^{-\frac{1}{2}} \|u_{h,*} - u\|_{L^2(0,T;L^2(\Omega_h))} + \|u\|_{L^2(0,T;L^2(\partial\Omega_h))} \\
&\leq C_{\text{tr}} h^{-\frac{1}{2}} c_p c_\Theta^{-1} \|u_{h,*} - u\|_{Z_h} + C_U \varrho_U \\
&\leq C_{\text{tr}} c_p c_\Theta^{-1} C_* \bar{h}^{\min\{p+\vartheta, p+1-\frac{\omega}{2}\}-\frac{1}{2}} + C_U \varrho_U.
\end{aligned} \tag{46}$$

Using an inverse inequality for the time derivative we have

$$\begin{aligned} \|\partial_t u_*\|_{L^2(0,T;L^2(\Omega))} &\leq C_{\text{inv}} \tau^{-1} \|u_{h,*} - u\|_{L^2(0,T;L^2(\Omega))} + \|\partial_t u\|_{L^2(0,T;L^2)} \\ &\leq C_{\text{inv}} \sqrt{c_r} c_p c_\Theta^{-1} C_* \bar{h}^{\min\{p+\vartheta-\omega, p+1-\frac{3\omega}{2}\}} + C_U \varrho_U. \end{aligned} \quad (47)$$

Using an inverse inequality for the time derivative and projection error estimate (39) we have

$$\begin{aligned} \|\partial_t(u_{h,*} - u_*)\|_{L^2(0,T;L^2(\Omega))} &\leq C_{\text{inv}} \tau^{-1} \|u_* - u_{h,*}\|_{L^2(0,T;L^2(\Omega))} \\ &\leq C_{\text{inv}} \sqrt{c_r} C_{\tilde{\pi}} T^{-\frac{1}{2}} \|u_*\|_V \bar{h}^{\min\{p+1,\nu\}-\omega} \end{aligned} \quad (48)$$

with $C_{\tilde{\pi}} > 0$ independent of h . Therefore, choosing \bar{h} , ϱ_U and ϱ_ℓ small enough, we get by combining estimates (44), (45), (46), (47), (48)

$$\kappa \lambda \| -\Gamma_*(b_h(u_{h,*}, \cdot) - \ell_h(\cdot)) \|_{Z_h}^\chi \leq \kappa^{1+\chi} \lambda \| b_h(u_{h,*}, \cdot) - \ell_h(\cdot) \|_{Z'_h}^\chi < \chi_0$$

independent of h .

Therefore, there exists a $\bar{h} > 0$ such that the required inequalities hold for any $u_{h,*} \in D_{\bar{h},*}$. We are now left to choose a starting value $u_{h,*}$ such that $B_\varrho^{Z_h}(u_{h,*}) \subseteq D_{*,\bar{h}}$ with ϱ from equation (41). For this we fix \bar{h} and let $u_{h,*} \in D_{h,*}$ with h to be chosen. Assuming that $v = \kappa \lambda \phi^\chi$ is below a certain threshold cf. (40), we have the bound

$$\varrho \leq 2\phi(1 - \kappa \lambda \phi^\chi) \leq 2\phi = 2\| -\Gamma(b_h(u_{h,*}, \cdot) - \ell_h(\cdot)) \|_{Z'_h}$$

so that ϱ can be made sufficiently small if h , ϱ_U and ϱ_ℓ are small enough by the previous estimates (44) to (47). Let $z_h \in B_\varrho^{Z_h}(u_{h,*})$. Then

$$\|z_h - u\|_{Z_h} \leq \|z_h - u_{h,*}\|_{Z_h} + \|u_{h,*} - u\|_{Z_h} \leq \varrho + C_* h^\xi,$$

so that choosing $\tilde{h} < \bar{h}$, ϱ_U and ϱ_ℓ so small such that $\varrho + C_* h^\xi < C_* \bar{h}^\xi$, we obtain $B_\varrho^{Z_h}(u_{h,*}) \subseteq D_{*,\bar{h}}$ for all $h < \tilde{h}$.

Applying Lemma 4.1 gives a unique $u_h \in B_{\tilde{\varrho}}^{Z_h}(u_{h,*}) \cap D_{h,*}$ with $\tilde{\varrho}$ from (41) such that $G_h(u_h) = 0$ for all $h < \tilde{h}$. Since $u_h \in D_{h,*}$, we automatically obtain the error estimate by construction. \square

Remark 4.1. *We note that the assumptions $\|u\|_U \leq \varrho_U$ and $\|\ell_h\|_{Z'_h} \leq \varrho_\ell$ can be fulfilled, if the data of the continuous problem (3) are chosen small enough, cf. [22]. Since uniform space-time methods are equivalent to time stepping methods, local existence of a discrete solution always holds if τ is chosen small enough. However, in Theorem 4.1 we show global in time well-posedness, in which case a convergence analysis without smallness assumptions (42) is not possible, since then global existence of the continuous solution u is not clear.*

Remark 4.2. *In comparison to Theorem 3.1 we can no longer take $p = 0$, since then the assumptions are not fulfilled. Taking $p = q = \omega = \vartheta = 1$ with $s = 2$, $\chi = \frac{1}{2}$ all assumptions are fulfilled and we obtain convergence if*

$$u \in H^2(0, T; H^1(\Omega; \mathbb{R}^{1+d})) \cap W^{2,\infty}(0, T; L^2(\Omega; \mathbb{R}^{1+d})) \cap C([0, T]; H^2(\Omega; \mathbb{R}^{1+d})).$$

A convergence analysis for less regular solutions is not contained in this paper.

5 Numerical experiments

For the numerical experiments, we aim to model sound waves propagating through soft tissue. To this end, we choose

$$\alpha = 1, \beta = 10^{-4}, \gamma = 6, \delta = 1, \varepsilon = 1, \zeta = 10^{-4}, \eta = 1, \theta = 1.$$

Since system (1) is in nondimensional form, most parameters are set to one. The value $\gamma = 6$ is derived from the nonlinearity parameter $\frac{B}{A} \approx 5$ in tissue, see [20] for details. The damping parameters are chosen to approximately match the viscosity coefficients observed in tissue. Due to computational constraints, we restrict our study to the case $d = 2$. The approximate domain $\Omega_h \times I_h$ is discretized using regular Lagrange quadrilateral elements with $4\tau = h$. The mesh is refined such that $h = 2^{-n_r}$, $n_r \geq 1$. We set the penalty constant to $C_\sigma = 50$. In our experiments, the linear systems to be solved exhibit a block-diagonal structure, so we solve them using GMRES in combination with a block Gauss–Seidel preconditioner. The implementation is carried out in M++, see [4], and can run in parallel. The complete source code is available at <https://gitlab.kit.edu/kit/mpp/mpp>.

5.1 Error indicator for p -adaptivity

In this paper, we only consider residual based adaptivity. We remark that a duality based adaptivity with respect to a goal functional is also possible, but not investigated in this paper. We apply p -adaptivity as a variant of the maximum marking strategy described in [12, Algorithm 1] and [40, Chapter 4.2], with the additional feature that derefinement is included. Thus, the degree of a space-time cell is increased if $\tilde{\varsigma}_R \geq \vartheta_{\text{ref}} \max_{R' \in \mathcal{R}_h} \tilde{\varsigma}_{R'}$ and decreased if $\tilde{\varsigma}_R \leq \vartheta_{\text{deref}} \max_{R' \in \mathcal{R}_h} \tilde{\varsigma}_{R'}$, depending on $\vartheta_{\text{ref}} > \vartheta_{\text{deref}} > 0$. In [12], for the problem $(M\partial_t + A)u = f$ the following local error estimator for a space-time cell $R = (I_j \times K)$ is used

$$\tilde{\varsigma}_R^2 = h \|(M\partial_t + A)u_h - f\|_{L^2(I \times K)}^2 + \frac{1}{2} \sum_{j=0}^k \|M^{\frac{1}{2}}[u_h]_j\|_{L^2(K)}^2 + \frac{1}{2} \int_I \|A_{\mathbf{n}}[u_h]\|_{L^2(\partial K)}^2 dt.$$

We, therefore, use the following error indicator to account for the nonlinear terms

$$\begin{aligned} \tilde{\varsigma}_R^2 &= h \|(M\partial_t + A)u_h + N(u_h, u_h) - f\|_{L^2(I \times K)}^2 \\ &\quad + \frac{1}{2} \sum_{j=0}^k \|M^{\frac{1}{2}}[u_h]_j\|_{L^2(K)}^2 + \frac{1}{2} \int_I \|A_{\mathbf{n}}[u_h]\|_{L^2(\partial K)}^2 dt \end{aligned}$$

and neglect diffusion terms, since they are small in our application. When advancing to the next refinement level, the coarse solution is used as the initial guess for Newton’s method. For each refined cell, both the temporal and spatial polynomial degrees are increased by one.

5.2 Known solution

For the first experiment, we choose the solution

$$u(t, x, y) = (\partial_t \psi, \partial_x \psi, \partial_y \psi) \quad \text{with} \quad \psi(t, x, y) = \psi_A \sin(\varphi t) \sin(kx) \sin(ky) \quad (49)$$

and set $\Omega = (0, 1)^2$, $I = (0, 1)$, $\Gamma_N = \emptyset$, $\psi_A = 0.01$, $\varphi = 6\pi$, $k = \pi$. In this setting, we have $\vartheta = \omega = 1$. Hence, Theorem 4.1 gives for $q = p = 1$ a convergence rate of $\xi = 1$, for $q = 1, p = 2$ a rate $\xi = \frac{3}{2}$ and for $p = q = 2$ we get the convergence rate $\xi = 2$.

When plotting the errors with respect to the DG-norm defined in (18) of the discrete solutions against the known solution u in (49), we observe that the actual convergence rates generally exceed the predictions of Theorem 4.1, see Figure 1. As expected, the L^2 errors are consistently smaller than the DG-norm errors.

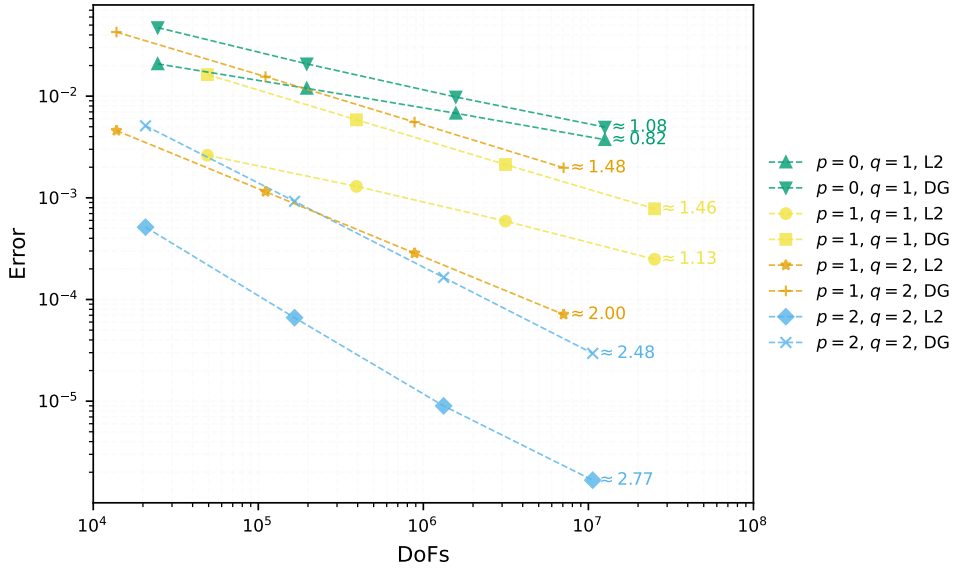


Figure 1: DG-norm error and L^2 space-time error comparison between known and discrete solutions for different time degrees p and space degrees q in dependence to the total degrees of freedom (DoFs) used. The extrapolated convergence order (ECO) is indicated at the right end of each line.

5.3 Unknown solution

For the next experiment, we set $\Omega = (-\frac{1}{2}, \frac{1}{2})^2$, $I = (0, 1)$, $\Gamma_N = \emptyset$ and assume homogeneous boundary conditions. As source terms, we choose a Gaussian bump excitation oscillating harmonically in time

$$p_S(t, x, y) = \begin{cases} a \exp(1) \sin(2\pi a_f t) \exp\left(-\frac{1}{1 - \frac{x^2 + y^2}{r_a^2}}\right), & \text{if } x^2 + y^2 < r_a^2, \\ 0, & \text{otherwise,} \end{cases}$$

for the pressure and set $v_S(t, x, y) = 0$. The initial conditions p_0, v_0 are set to zero and as parameters we choose $a = 2$, $a_f = 3$, and $r_a = 0.2$. Fig. 2 and 3 show the pressure variable of the numerical solution at different time steps. As expected, the solution is radially symmetric.

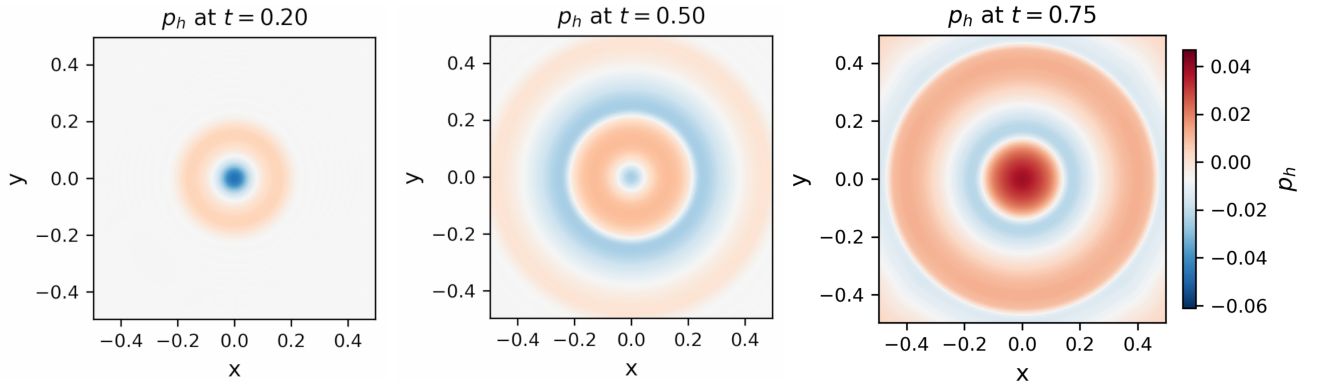


Figure 2: Numerical solution for $n_r = 7$ and $p = q = 1$ at different time steps. The approximated pressure p_h is plotted.

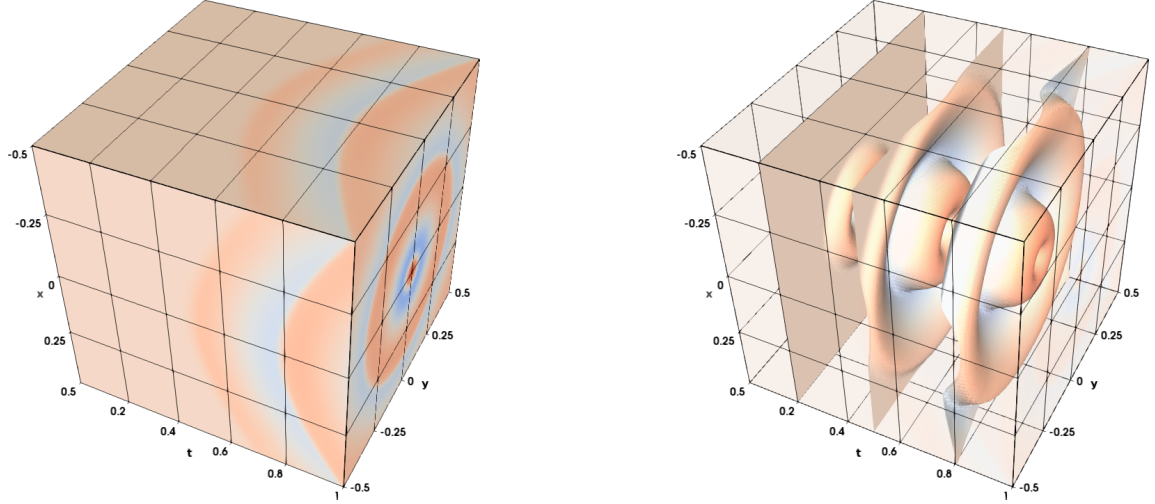


Figure 3: Numerical solution p_h for $n_r = 7$ and $p = q = 1$ on the space-time domain.

We first note that the model successfully reproduces the characteristic waveform observed in nonlinear acoustics, including the generation of higher harmonics at integer multiples of the base frequency $a_f = 3$, see Figure 4. To compare the linear and nonlinear behavior of the system, we compute, for $n_r = 7$ and $p = q = 1$, the numerical solution u_h of the full nonlinear model and the corresponding solution

u_h^L obtained by setting $\gamma = \delta = \eta = \theta = 0$. To analyze the harmonic content, we evaluate the discrete Fourier transform \mathcal{F}_h of the pressure signals.

Since the source p_s has a base frequency $a_f = 3$, additional spectral components appear at frequencies $\omega_F = 3, 6, 9, \dots$, indicating the presence of nonlinear harmonic generation in the full model. We also observe the well known behavior that the nonlinear wave exhibits a shift in its peak values, corresponding to a local change in sound speed. Namely, peaks occur earlier than in the linear wave when the amplitude is positive, and later when the amplitude is negative.

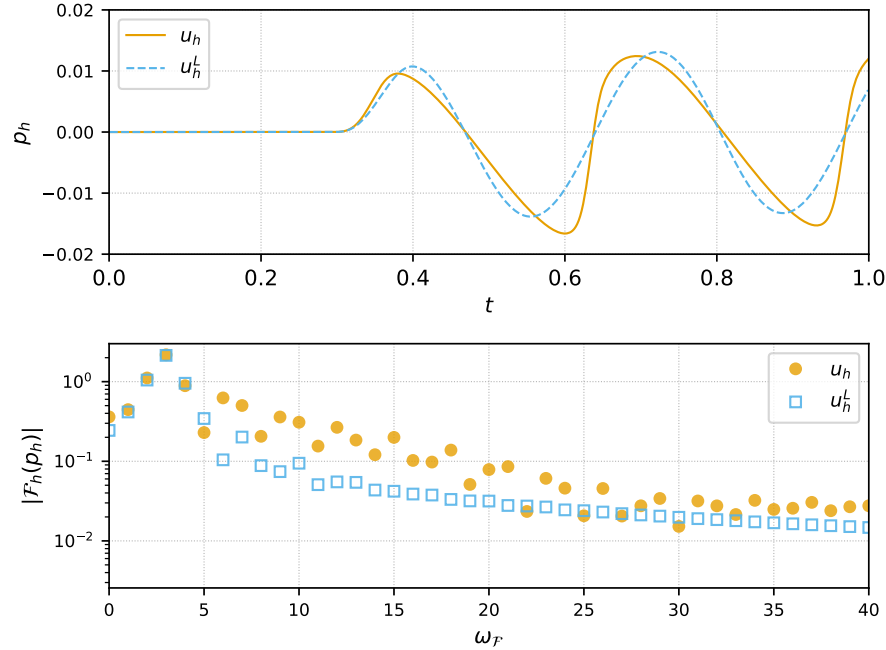


Figure 4: At the top, the time evolution of the pressure at $(x, y) = (0.246094, 0.246094)$ is shown. The blue dotted line corresponds to the pressure component of the solution $u_h^L = (p_h^L, v_h^L)$ obtained with $\gamma = \delta = \eta = \theta = 0$, while the orange solid line represents the pressure from the full nonlinear model. At the bottom, the corresponding magnitudes of the discrete Fourier transforms of p_h and p_h^L are displayed.

To test the adaptivity and the error estimator described above, we plot the error estimator $\tilde{\zeta}_R$ in the L^2 norm for each iteration and for different values of n_r in dependence of the total degrees of freedoms used in Figure 5. We perform two refinement steps, starting with initial space-time degrees of $p = 0, q = 1$ and $p = q = 1$. The marking parameter ϑ_{ref} is set to 10^{-1} and the derefinement parameter $\vartheta_{\text{deref}} = 10^{-2}$. We observe that the error estimator decays within each refinement in all cases, except for $p = 1, q = 1, n_r = 6$.

Next, in order to test convergence, we evaluate the functionals

$$P(p)[t] := \int_{\Omega} p(t) \, dx \text{ and } E(v)[t] := \int_{\Omega} v(t) \cdot v(t) \, dx$$

numerically at each time point and compute the L^1 and L^2 errors in time. Since the exact solution is unknown, we use a discrete reference solution $u_h^R = (p_h^R, v_h^R)$ computed with $p = q = 1$ and $n_r = 7$. The results for the functionals P and E are shown in the Tables 1, 2 as well as in the Figures 6 and 7, respectively. Overall, we observe convergence of the functionals toward the values evaluated at the discrete reference solution. However, we note that adaptivity only becomes advantageous for relatively high numbers of degrees of freedom, around 10^7 . We also observe the tendency that adaptivity approximates E more effectively than P .

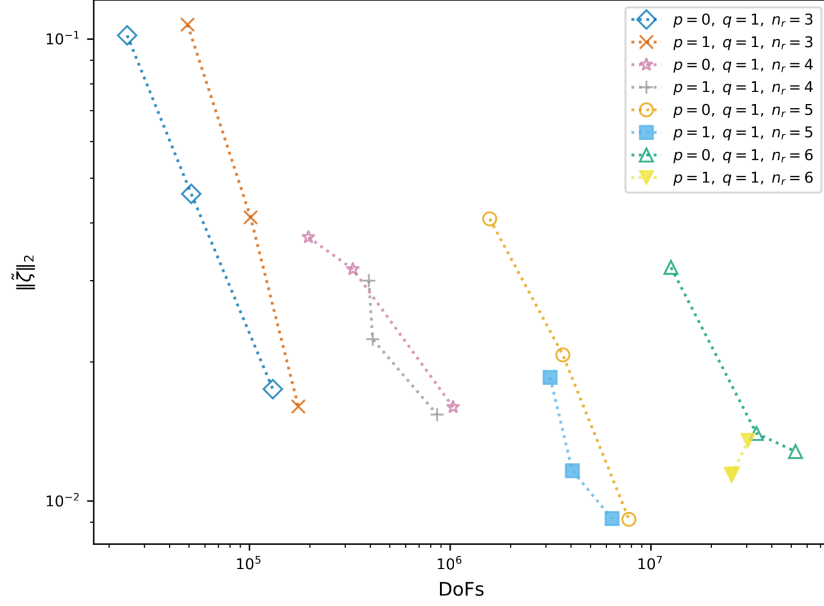


Figure 5: The L^2 norm of the nonlinear global error estimator $\tilde{\zeta}$ is shown in dependence of the degree of freedoms of each adaptive iteration.

cells	$p = q = 1$			$p = q = 2$		
	DoF	$\ P(e_h)\ _1$	$\ E(e_h)\ _2$	DoF	$\ P(e_h)\ _1$	$\ E(e_h)\ _2$
2 048	49 150	1.67613	0.17467	165 900	0.47892	0.02186
16 380	393 200	0.36469	0.04925	1 327 000	0.16742	0.00780
131 100	3 146 000	0.21867	0.02271	10 620 000	0.10059	0.01722
1 049 000	25 170 000	0.06514	0.01115	84 930 000	0.08683	0.00636
EOC		1.562	1.323		0.821	0.594

Table 1: Approximation errors of P, E and extrapolated order of convergence (EOC) for $p = q = 1$ and $p = q = 2$.

cells	adaptive $p = 0, q = 1$			adaptive $p = q = 1$		
	DoF	$\ P(e_h)\ _1$	$\ E(e_h)\ _2$	DoF	$\ P(e_h)\ _1$	$\ E(e_h)\ _2$
2 048	130 700	0.47985	0.08535	175 100	0.51269	0.08465
16 380	1 034 000	0.21338	0.03840	860 500	0.22487	0.03840
131 100	7 769 000	0.08215	0.00803	6 403 000	0.07407	0.00808
1 049 000	52 490 000	0.05237	0.00312	30 430 000	0.02869	0.00331
EOC		1.1016	1.656		1.656	1.846

Table 2: Approximation errors of P, E and extrapolated order of convergence (EOC) for adaptive runs starting with $p = 0, q = 1$ and $p = q = 1$.

In Tab. 1 and Tab. 2 the extrapolated order of convergence is investigated for the weighted errors $\|P(e_h)\|_1 = 10^4 \int_0^T |P(p_h) - P(p_h^R)| dt$ and $\|E(e_h)\|_2 = 10^4 \left(\int_0^T (E(v_h) - E(v_h^R))^2 dt \right)^{\frac{1}{2}}$.

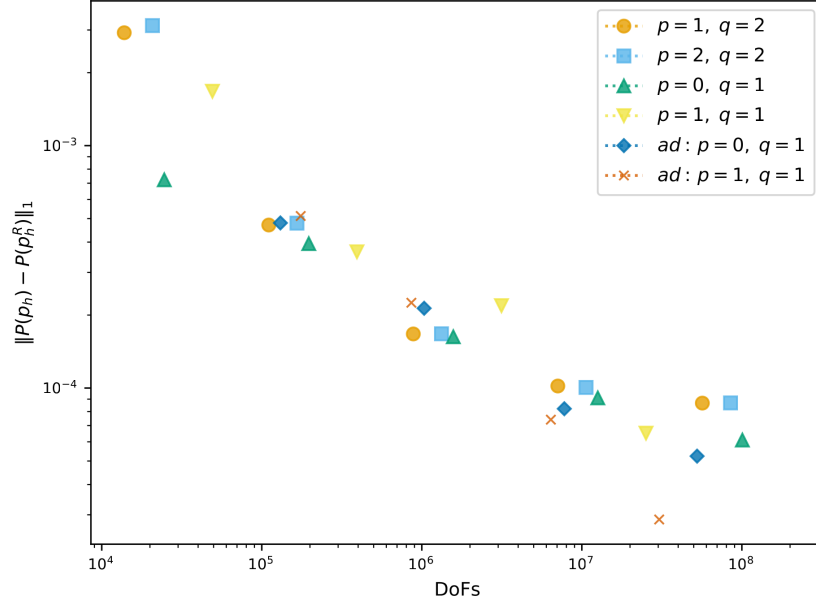


Figure 6: Convergence to the functional P in the L^1 norm is shown in dependence of the degrees of freedom of each solution. For adaptive solutions the last iteration is used.

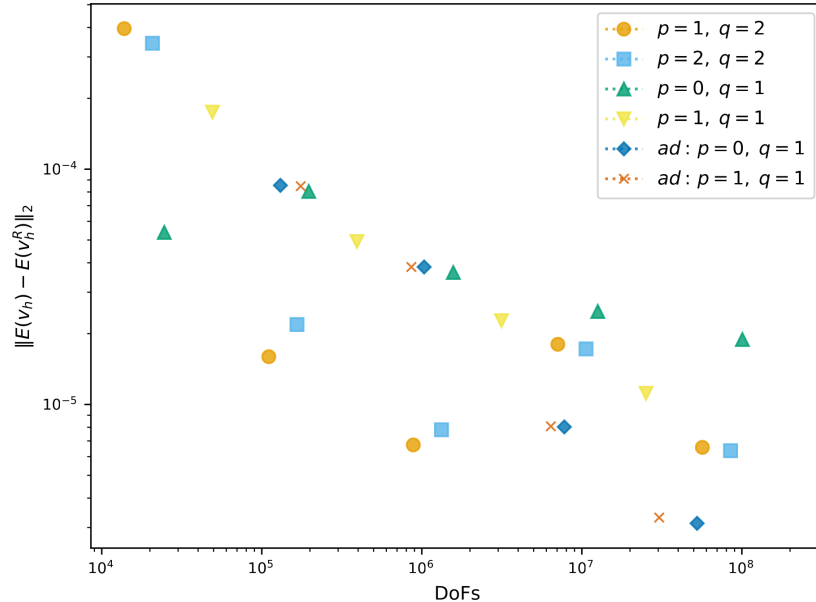


Figure 7: Convergence to the functional E in the L^2 norm is shown in dependence of the degrees of freedom of each solution. For adaptive solutions the last iteration is used.

6 Conclusion

In this work, we have developed a space-time DG method for a nonlinear acoustic equation, extending the framework of linear symmetric Friedrichs systems. We have rigorously established the well-posedness of the scheme and proved convergence in the natural DG norm. Numerical experiments confirm the theoretical results and illustrate the potential of p -adaptivity for improving accuracy. While adaptivity shows benefits for high resolution cases, its effectiveness at moderate resolutions remains limited, highlighting the need for further investigation and optimization. Overall, the proposed approach provides a robust and flexible framework for the numerical simulation of nonlinear acoustic waves, paving the way for future studies.

A mathematically rigorous convergence analysis of the p -adaptive algorithm is beyond the scope of this paper and remains an open question in the literature. Future investigations could explore hp -adaptive algorithms or hybrid DG methods to further enhance efficiency.

Acknowledgment

The authors thank Barbara Kaltenbacher for her careful reading of the manuscript and helpful suggestions, which have led to marked improvements. This research was funded in whole or in part by the Austrian Science Fund (FWF) [10.55776/P36318]. For open access purposes, the author has applied a CC BY public copyright license to any author accepted manuscript version arising from this submission.

References

- [1] P. F. Antonietti, I. Mazzieri, M. Muhr, V. Nikolić, and B. Wohlmuth. A high-order discontinuous Galerkin method for nonlinear sound waves. *Journal of Computational Physics*, 415:109484, 2020.
- [2] P.F. Antonietti, I. Mazzieri, and F. Migliorini. A space-time discontinuous Galerkin method for the elastic wave equation. *Journal of Computational Physics*, 419:109685, 2020.
- [3] W. Barham and P. J. Morrison. A mimetic discretization of Westervelt's equation. *arXiv preprint arXiv:2407.14718*, 2024. Available at <https://arxiv.org/abs/2407.14718>.
- [4] N. Baumgarten and C. Wieners. The parallel finite element system M++ with integrated multi-level preconditioning and multilevel Monte Carlo methods. *Computers & Mathematics with Applications*, 81:391–406, 2021. Development and Application of Open-source Software for Problems with Numerical PDEs.
- [5] S. C. Brenner. Poincaré–Friedrichs Inequalities for Piecewise H^1 Functions. *SIAM Journal on Numerical Analysis*, 41(1):306–324, 2003.
- [6] M. Campo-Valera, D. Diego-Tortosa, R. Asorey-Cacheda, J. L. Gómez-Tornero, and L. J. Herrera-Fernández. A novel modulation approach based on nonlinear acoustic signals for underwater communications. In *Proceedings of the 10th Convention of the European Acoustics Association (Forum Acusticum 2023)*, pages 1–4, Turin, Italy, 2023. European Acoustics Association.

- [7] A. Cangiani, Z. Dong, and E. H. Georgoulis. *hp*-Version Space-Time Discontinuous Galerkin Methods for Parabolic Problems on Prismatic Meshes. *SIAM Journal on Scientific Computing*, 39(4):A1251–A1279, 2017.
- [8] D. Corallo, W. Dörfler, and C. Wieners. Space-Time Discontinuous Galerkin Methods for Weak Solutions of Hyperbolic Linear Symmetric Friedrichs Systems. *J Sci Comput*, 94(1):27, 2022.
- [9] P. Deuflhard. *Newton Methods for Nonlinear Problems: Affine Invariance and Adaptive Algorithms*. Springer Series in Computational Mathematics. Springer Berlin Heidelberg, 2011.
- [10] D.A. Di Pietro and A. Ern. *Mathematical Aspects of Discontinuous Galerkin Methods*. Mathématiques et Applications. Springer Berlin Heidelberg, 2011.
- [11] V. Dolejší and M. Feistauer. *Discontinuous Galerkin Method: Analysis and Applications to Compressible Flow*, volume 48 of *Springer Series in Computational Mathematics*. Springer International Publishing, Cham, 2015.
- [12] W. Dörfler, S. Findeisen, C. Wieners, and D. Ziegler. *Parallel adaptive discontinuous Galerkin discretizations in space and time for linear elastic and acoustic waves*, pages 61–88. De Gruyter, Berlin, Boston, 2019.
- [13] B. Dörich and V. Nikolić. Robust fully discrete error bounds for the Kuznetsov equation in the inviscid limit. *arXiv preprint arXiv:2401.06492*, 2024. Available at <https://arxiv.org/abs/2401.06492>.
- [14] H. Egger and M. Fritz. Well-posedness, long-time behavior, and discretization of some models of nonlinear acoustics in velocity–enthalpy formulation. *Mathematical Methods in the Applied Sciences*, 48(1):1–22, 2025.
- [15] L.C. Evans. *Partial Differential Equations*, volume 19 of *Graduate Studies in Mathematics*. American Mathematical Society, Providence (R.I.), second edition, 2010.
- [16] G.P. Malfense Fierro, F. Ciampa, D. Ginzburg, E. Onder, and M. Meo. Nonlinear ultrasound modelling and validation of fatigue damage. *Journal of Sound and Vibration*, 343:121–130, 2015.
- [17] S. Gómez and M. Meliani. Asymptotic-preserving hybridizable discontinuous Galerkin method for the Westervelt quasilinear wave equation. *arXiv preprint arXiv:2405.03535*, 2024. Available at <https://arxiv.org/abs/2405.03535>.
- [18] S. Gómez and A. Moiola. A space–time DG method for the Schrödinger equation with variable potential. *Advances in Computational Mathematics*, 50(2):Article 15, 2024.
- [19] S. Gómez and V. Nikolić. Combined DG-CG finite element method for the Westervelt equation. *arXiv preprint arXiv:2412.09095*, 2024. Available at <https://arxiv.org/abs/2412.09095>.
- [20] M.F. Hamilton and D.T. Blackstock. *Nonlinear Acoustics*. Academic Press, San Diego, Calif., first edition, 1997.
- [21] M. A. Hernández. The Newton method for operators with Hölder continuous first derivative. *Journal of Optimization Theory and Applications*, 109(3):631–648, 2001.
- [22] B. Kaltenbacher and P. Lehner. A first order in time wave equation modeling nonlinear acoustics. *Journal of Mathematical Analysis and Applications*, 543(2, Part 2):128933, 2025.

- [23] B. Kaltenbacher, V. Nikolić, and M. Thalhammer. Efficient time integration methods based on operator splitting and application to the Westervelt equation. *IMA Journal of Numerical Analysis*, 35(3):1092–1124, 2015.
- [24] E. Karabelas. *Space-Time Discontinuous Galerkin Methods for Cardiac Electromechanics*, volume 28 of *Monographic Series TU Graz, Computation in Engineering Science (CES)*. Verlag der Technischen Universität Graz, Graz, 2016.
- [25] C.M. Klaij, J.J.W. van der Vegt, and H. van der Ven. Space–time discontinuous Galerkin method for the compressible Navier–Stokes equations. *Journal of Computational Physics*, 217(2):589–611, 2006.
- [26] V. P. Kuznetsov. Equations of nonlinear acoustics. *Soviet Physics: Acoustics*, (16):467–470, 1971.
- [27] U. Langer and O. Steinbach, editors. *Space-Time Methods*. De Gruyter, Berlin, Boston, 2019.
- [28] A. Lasis and E. Süli. Poincaré-type inequalities for broken Sobolev spaces. *Evolution Equations & Control Theory*, 4(4):447–491, 2003.
- [29] P. Lehner. Well-posedness of a first-order-in-time model for nonlinear acoustics with nonhomogeneous boundary conditions. *Nonlinear Analysis: Real World Applications*, 91:104609, 2026.
- [30] A. Moiola and I. Perugia. A space-time Trefftz discontinuous Galerkin method for the acoustic wave equation in first-order formulation. *Numer. Math.*, 138(2):389–435, 2018.
- [31] M. Muhr, V. Nikolić, and B. Wohlmuth. A discontinuous Galerkin coupling for nonlinear elasto-acoustics. *IMA Journal of Numerical Analysis*, 43(1):225–257, 2023.
- [32] V. Nikolić and B. Wohlmuth. A priori error estimates for the finite element approximation of Westervelt’s quasi-linear acoustic wave equation. *SIAM Journal on Numerical Analysis*, 57(4):1897–1918, 2019.
- [33] G. V. Norton and R. D. Purrington. The Westervelt equation with viscous attenuation versus a causal propagation operator: A numerical comparison. *Journal of Sound and Vibration*, 327(1–2):163–172, 2009.
- [34] S. Rhebergen, B. Cockburn, and J. J.W. van der Vegt. A space–time discontinuous Galerkin method for the incompressible Navier–Stokes equations. *Journal of Computational Physics*, 233:339–358, 2013.
- [35] O. V. Rudenko. Nonlinear Acoustics in Medicine: A Review. *Physics of Wave Phenomena*, 30(2):73–85, 2022.
- [36] O. A. Sapozhnikov, V. A. Khokhlova, R. O. Cleveland, P. Blanc-Benon, and M. F. Hamilton. Nonlinear acoustics today. *Acoustics Today*, 15(3):55–64, 2019.
- [37] M. Tavelli and M. Dumbser. A staggered space–time discontinuous Galerkin method for the three-dimensional incompressible Navier–Stokes equations on unstructured tetrahedral meshes. *Journal of Computational Physics*, 319:294–323, 2016.
- [38] R. Velasco-Segura and P. L. Rendón. A finite volume approach for the simulation of nonlinear dissipative acoustic wave propagation. *Wave Motion*, 58:180–195, 2015. Available online 21 May 2015.

- [39] P. J. Westervelt. Parametric acoustic array. *The Journal of the Acoustical Society of America*, 35(4):535–537, 1963.
- [40] D. Ziegler. *A Parallel and Adaptive Space-Time Discontinuous Galerkin Method for Visco-Elastic and Visco-Acoustic Waves*. Dissertation, Karlsruhe Institute of Technology (KIT), Karlsruhe, Germany, 2019.

A Details to upwind flux

In order to obtain an expression for the upwind flux (9) $A_{\mathbf{n}_K}^{\text{up}}$ of

$$\begin{aligned}\alpha \partial_t p + \nabla \cdot \mathbf{v} &= p_S \\ \varepsilon \partial_t \mathbf{v} + \nabla p &= \mathbf{v}_S,\end{aligned}$$

we follow along the lines of the theory presented in [12, Section 3] and assume $d = 2$ for simplicity. In its general form, the Friedrichs system can be written as

$$(M \partial_t + A)u = f$$

defined on $\Omega \subset \mathbb{R}^2$, where

$$M = \begin{pmatrix} \alpha & 0 & 0 \\ 0 & \varepsilon & 0 \\ 0 & 0 & \varepsilon \end{pmatrix}$$

and $A = A_1 \partial_{x_1} + A_2 \partial_{x_2}$ with

$$A_1 = \begin{pmatrix} 0 & 1 & 0 \\ 1 & 0 & 0 \\ 0 & 0 & 0 \end{pmatrix}, \quad A_2 = \begin{pmatrix} 0 & 0 & 1 \\ 0 & 0 & 0 \\ 1 & 0 & 0 \end{pmatrix}, \quad A_{\mathbf{n}} = n_1 A_1 + n_2 A_2 = \begin{pmatrix} 0 & n_1 & n_2 \\ n_1 & 0 & 0 \\ n_2 & 0 & 0 \end{pmatrix}.$$

To construct $A_{\mathbf{n}_K}^{\text{up}}$, we use the nontrivial eigenpairs of $M^{-1}A_{\mathbf{n}}$ fulfilling $A_{\mathbf{n}}w = \lambda Mw$ with $\lambda \in \mathbb{R}$ and $w \in \mathbb{R}^3$. Writing $c_0 := \sqrt{\alpha^{-1}\varepsilon^{-1}}$ these are

$$\lambda_{2,3} = \pm c_0, \quad w_{2,3} = \begin{pmatrix} \alpha^{-1} \\ \pm c_0 \mathbf{n} \end{pmatrix}.$$

According to [12], $A_{\mathbf{n}_K}^{\text{up}}$ is then given as

$$A_{\mathbf{n}_K}^{\text{up}} y = A_{\mathbf{n}_K}^- y$$

with

$$\begin{aligned}A_{\mathbf{n}}^- y &= \lambda_3 \frac{w_3 \cdot M y}{w_3 \cdot M w_3} M w_3 = \frac{-c}{\alpha^{-1} + \varepsilon c_0^2} \begin{pmatrix} 1 \\ -\varepsilon c_0 \mathbf{n} \end{pmatrix} (y_1 - c_0 \varepsilon \mathbf{n} \cdot (y_2, y_3)) \\ &= \frac{-1}{\alpha^{-1} c_0^{-1} + \varepsilon c_0} \begin{pmatrix} 1 \\ -\varepsilon c_0 \mathbf{n} \end{pmatrix} (y_1 - c_0 \varepsilon \mathbf{n} \cdot (y_2, y_3)) \\ &= \frac{-1}{2\sqrt{\alpha^{-1}\varepsilon}} \begin{pmatrix} 1 \\ -\varepsilon c_0 \mathbf{n} \end{pmatrix} (y_1 - c_0 \varepsilon \mathbf{n} \cdot (y_2, y_3)).\end{aligned}$$

Therefore, writing $Z_0 = \sqrt{\alpha^{-1}\varepsilon}$ for the acoustic impedance, we get

$$A_{\mathbf{n}_K}^{\text{up}} \begin{pmatrix} [p]_{F,K} \\ [v]_{F,K} \end{pmatrix} = -\frac{1}{2Z_0} ([p]_{F,K} - Z_0 [v]_{F,K} \cdot \mathbf{n}_K) \begin{pmatrix} 1 \\ -Z_0 \mathbf{n}_K \end{pmatrix}.$$

This yields the matrix

$$A_{\mathbf{n}_K}^{\text{up}} = \frac{1}{2} \begin{pmatrix} -\frac{1}{Z_0} & \mathbf{n}_K^\top \\ \mathbf{n}_K & -Z_0 \mathbf{n}_K \mathbf{n}_K^\top \end{pmatrix} = A_D + \frac{1}{2} A_{\mathbf{n}_K} \text{ with } A_D = \frac{1}{2} \begin{pmatrix} -\frac{1}{Z_0} & 0 \\ 0 & -Z_0 \mathbf{n}_K \mathbf{n}_K^\top \end{pmatrix},$$

as in (9).

Lemma A.1. *We have for all $u_h \in Z_h$*

$$a_h(u_h, u_h) = \frac{1}{2} \sum_{K \in \mathcal{K}_h} \left(\sum_{F \in \mathcal{F}_K} \|\sqrt{-A_D}[u_h]_{F,K}\|_F^2 \right).$$

Proof. By partial integration we have for all $K \in \mathcal{K}_h$

$$(Au_h, z_h)_K + (u_h, Az_h)_K = (A_{\mathbf{n}_K} u_h, z_h)_{\partial K},$$

which corresponds to the skew-adjointness of A . Setting $z_h = u_h$ yields

$$(Au_h, u_h)_K = \frac{1}{2} (A_{\mathbf{n}_K} u_h, u_h)_{\partial K} = \frac{1}{2} \sum_{F \in \mathcal{F}_K} (A_{\mathbf{n}_K} u_{h,K}, u_{h,K})_F = \sum_{F \in \mathcal{F}_K} (p_{h,K}, v_{h,K} \cdot \mathbf{n}_K)_F. \quad (50)$$

For inner faces we have

$$\begin{aligned} & \frac{1}{2} \sum_{K \in \mathcal{K}_h} \sum_{F \in \mathcal{F}_K \cap \Omega} \|\sqrt{-A_D}[u_h]_{F,K}\|_{L^2(F)}^2 \\ &= \sum_{K \in \mathcal{K}_h} \sum_{F \in \mathcal{F}_K \cap \Omega} \frac{1}{2} (-A_D[u_h]_{F,K}, [u_h]_{F,K})_F \\ &= \sum_{K \in \mathcal{K}_h} \sum_{F \in \mathcal{F}_K \cap \Omega} \left(\frac{1}{2} A_D[u_h]_{F,K}, u_{h,K} - u_{h,K_F} \right)_F \\ &= \sum_{K \in \mathcal{K}_h} \sum_{F \in \mathcal{F}_K \cap \Omega} \left(\frac{1}{2} A_D[u_h]_{F,K}, u_{h,K} - u_{h,K_F} \right)_F + \left(\frac{1}{2} A_D[u_h], u_{h,K} \right)_F - \left(\frac{1}{2} A_D[u_h], u_{h,K} \right)_F \\ &= \sum_{K \in \mathcal{K}_h} \sum_{F \in \mathcal{F}_K \cap \Omega} (A_D[u_h]_{F,K}, u_{h,K})_F - \left(\frac{1}{2} A_D[u_h]_{F,K}, u_{h,K_F} \right)_F - \left(\frac{1}{2} A_D[u_h], u_{h,K} \right)_F \\ &= \sum_{K \in \mathcal{K}_h} \sum_{F \in \mathcal{F}_K \cap \Omega} (A_D[u_h]_{F,K}, u_{h,K})_F \\ &= \sum_{K \in \mathcal{K}_h} \sum_{F \in \mathcal{F}_K \cap \Omega} (A_D[u_h]_{F,K}, u_{h,K})_F + \frac{1}{2} (A_{\mathbf{n}_K}[u_h]_{F,K}, u_{h,K}) - \frac{1}{2} (A_{\mathbf{n}_K}[u_h]_{F,K}, u_{h,K}) \\ &= \sum_{K \in \mathcal{K}_h} \sum_{F \in \mathcal{F}_K \cap \Omega} (A_{\mathbf{n}_K}^{\text{up}}[u_h]_{F,K}, u_{h,K})_F - \frac{1}{2} (A_{\mathbf{n}_K}[u_h]_{F,K}, u_{h,K}) \\ &= \sum_{K \in \mathcal{K}_h} \sum_{F \in \mathcal{F}_K \cap \Omega} (A_{\mathbf{n}_K}^{\text{up}}[u_h]_{F,K}, u_{h,K})_F + \frac{1}{2} (A_{\mathbf{n}_K} u_{h,K}, u_{h,K})_F - \frac{1}{2} (A_{\mathbf{n}_K} u_{h,K_F}, u_{h,K})_F \\ &= \sum_{K \in \mathcal{K}_h} \sum_{F \in \mathcal{F}_K \cap \Omega} (A_{\mathbf{n}_K}^{\text{up}}[u_h]_{F,K}, u_{h,K})_F + \frac{1}{2} (A_{\mathbf{n}_K} u_{h,K}, u_{h,K})_F. \end{aligned} \quad (51)$$

From definition (10), we have in the Dirichlet case

$$\begin{aligned}
& \sum_{K \in \mathcal{K}_h} \sum_{F \in \mathcal{F}_K \cap \Gamma_D} \|\sqrt{-A_D}[u_h]_{F,K}\|_{L^2(F)}^2 \\
&= \sum_{K \in \mathcal{K}_h} \sum_{F \in \mathcal{F}_K \cap \Gamma_D} (-A_D[u_h]_{F,K}, [u_h]_{F,K})_F \\
&= \sum_{K \in \mathcal{K}_h} \sum_{F \in \mathcal{F}_K \cap \Gamma_D} (-A_D u_{h,F}, u_{h,F})_F \\
&= \sum_{K \in \mathcal{K}_h} \sum_{F \in \mathcal{F}_K \cap \Gamma_D} (-A_D u_{h,F}, u_{h,F})_F - \frac{1}{2}(A_{\mathbf{n}_K} u_{h,F}, u_{h,F})_F + \frac{1}{2}(A_{\mathbf{n}_K} u_{h,F}, u_{h,F})_F \\
&= \sum_{K \in \mathcal{K}_h} \sum_{F \in \mathcal{F}_K \cap \Gamma_D} (A_{\mathbf{n}_K}^{\text{up}}[u_h]_{F,K}, u_{h,K})_F + \frac{1}{2}(A_{\mathbf{n}_K} u_{h,F}, u_{h,F})_F
\end{aligned} \tag{52}$$

and in the Neumann case

$$\begin{aligned}
& \frac{1}{2} \sum_{K \in \mathcal{K}_h} \sum_{F \in \mathcal{F}_K \cap \Gamma_N} \|\sqrt{-A_D}[u_h]_{F,K}\|_{L^2(F)}^2 \\
&= \sum_{K \in \mathcal{K}_h} \sum_{F \in \mathcal{F}_K \cap \Gamma_N} \frac{1}{2} (-A_D[u_h]_{F,K}, [u_h]_{F,K})_F \\
&= \sum_{K \in \mathcal{K}_h} \sum_{F \in \mathcal{F}_K \cap \Gamma_N} (-2A_D(0, v_{h,F})^\top, u_{h,F})_F \\
&= \sum_{K \in \mathcal{K}_h} \sum_{F \in \mathcal{F}_K \cap \Gamma_N} (-2A_D(0, v_{h,F})^\top, u_{h,F})_F - (A_{\mathbf{n}_K}(0, v_{h,F})^\top, u_{h,F})_F + \frac{1}{2}(A_{\mathbf{n}_K} u_{h,F}, u_{h,F})_F \\
&= \sum_{K \in \mathcal{K}_h} \sum_{F \in \mathcal{F}_K \cap \Gamma_N} (A_{\mathbf{n}_K}^{\text{up}}[u_h]_{F,K}, u_{h,K})_F + \frac{1}{2}(A_{\mathbf{n}_K} u_{h,F}, u_{h,F})_F.
\end{aligned} \tag{53}$$

In total, combining (51), (52), (53), and using skew-adjointness of A (50), we obtain

$$\begin{aligned}
& \frac{1}{2} \sum_{K \in \mathcal{K}_h} \left(\sum_{F \in \mathcal{F}_K} \|\sqrt{-A_D}[u_h]_{F,K}\|_F^2 \right) \\
&= \sum_{K \in \mathcal{K}_h} \left(\sum_{F \in \mathcal{F}_K} (A_{\mathbf{n}_K}^{\text{up}}[u_h]_{F,K}, u_{h,K})_F + \frac{1}{2}(A_{\mathbf{n}_K} u_{h,F}, u_{h,F})_F \right) \\
&= \sum_{K \in \mathcal{K}_h} \left((Au_h, u_h)_K + \sum_{F \in \mathcal{F}_K} (A_{\mathbf{n}_K}^{\text{up}}[u_h]_{F,K}, u_{h,K})_F \right) = a_h(u_h, u_h).
\end{aligned} \tag{54}$$

□

To obtain an estimate as (11), we note that

$$\sqrt{-A_D} = \frac{1}{\sqrt{2}} \begin{pmatrix} \frac{1}{\sqrt{Z_0}} & 0 \\ 0 & \sqrt{Z_0} \mathbf{n}_K \mathbf{n}_K^\top \end{pmatrix},$$

since $\sqrt{\mathbf{n}_K \mathbf{n}_K^\top} = \mathbf{n}_K \mathbf{n}_K^\top$. Thus,

$$\| -\sqrt{A_D} u \|_{L^2(F)}^2 = \frac{1}{2Z_0} \|p\|_{L^2(F)}^2 + \frac{Z_0}{2} \|v \cdot n\|_{L^2(F)}^2$$

together with

$$\|A_{\mathbf{n}_K} u\|_{L^2(F)}^2 = \|p\|_{L^2(F)}^2 + \|v \cdot n\|_{L^2(F)}^2$$

gives us

$$2 \min\left\{\frac{1}{Z_0}, Z_0\right\} \|A_{\mathbf{n}_K} u\|_{L^2(F)}^2 \leq \|\sqrt{-A_D} u\|_{L^2(F)}^2 \leq \frac{1}{2} \max\left\{\frac{1}{Z_0}, Z_0\right\} \|A_{\mathbf{n}_K} u\|_{L^2(F)}^2.$$

Therefore, due to equation (54), we see that estimate (11) holds with $c_A = 4 \min\left\{\frac{1}{Z_0}, Z_0\right\}$ and $C_A = \frac{1}{4} \max\left\{\frac{1}{Z_0}, Z_0\right\}$.

Lemma A.2. *For all $u_h \in Z_h + U$ and $z_h \in Z_h$ we have*

$$\sum_{K \in \mathcal{K}_h} \sum_{F \in \mathcal{F}_K} (A_{\mathbf{n}_K}^{up} [u_h]_{F,K}, z_{h,K})_F = \sum_{K \in \mathcal{K}_h} \sum_{F \in \mathcal{F}_K} (u_{h,K}, A_{\mathbf{n}_K}^{up} [z_h]_{F,K})_F.$$

Proof. First of all, we note that $-A_{\mathbf{n}_K}^{up}$ has eigenpairs

$$0, \begin{pmatrix} Z_0 n_1 \\ 1 \\ 0 \end{pmatrix} \quad 0, \begin{pmatrix} Z_0 n_2 \\ 0 \\ 1 \end{pmatrix} \quad \frac{1}{2} \left(Z_0 + \frac{1}{Z_0} \right), \begin{pmatrix} -\frac{1}{Z_0} \\ n_1 \\ n_2 \end{pmatrix}.$$

Therefore, it is possible to choose a square root of $-A_{\mathbf{n}_K}^{up}$. For inner faces, due to the symmetry of $A_{\mathbf{n}_K}^{up}$, we have

$$\begin{aligned} & \sum_{K \in \mathcal{K}_h} \sum_{F \in \mathcal{F}_K \cap \Omega} (A_{\mathbf{n}_K}^{up} [u_h]_{F,K}, z_{h,K})_F \\ &= \sum_{K \in \mathcal{K}_h} \sum_{F \in \mathcal{F}_K \cap \Omega} ([u_h]_{F,K}, A_{\mathbf{n}_K}^{up} z_{h,K})_F + (u_{h,K}, A_{\mathbf{n}_K}^{up} z_{h,K_F})_F - (u_{h,K}, A_{\mathbf{n}_K}^{up} z_{h,K_F})_F \\ &= \sum_{K \in \mathcal{K}_h} \sum_{F \in \mathcal{F}_K \cap \Omega} (u_{h,K}, A_{\mathbf{n}_K}^{up} [z_h]_{F,K})_F + (u_{h,K_F}, A_{\mathbf{n}_K}^{up} z_{h,K})_F - (u_{h,K}, A_{\mathbf{n}_K}^{up} z_{h,K_F})_F \\ &= \sum_{K \in \mathcal{K}_h} \sum_{F \in \mathcal{F}_K \cap \Omega} (u_{h,K}, A_{\mathbf{n}_K}^{up} [z_h]_{F,K})_F - (u_{h,K_F}, -A_{\mathbf{n}_K}^{up} z_{h,K})_F + (u_{h,K}, -A_{\mathbf{n}_K}^{up} z_{h,K_F})_F \\ &= \sum_{K \in \mathcal{K}_h} \sum_{F \in \mathcal{F}_K \cap \Omega} (u_{h,K}, A_{\mathbf{n}_K}^{up} [z_h]_{F,K})_F - (\sqrt{-A_{\mathbf{n}_K}^{up}} u_{h,K_F}, \sqrt{-A_{\mathbf{n}_K}^{up}} z_{h,K})_F \\ & \quad + (\sqrt{-A_{\mathbf{n}_K}^{up}} u_{h,K}, \sqrt{-A_{\mathbf{n}_K}^{up}} z_{h,K_F})_F \\ &= \sum_{K \in \mathcal{K}_h} \sum_{F \in \mathcal{F}_K \cap \Omega} (u_{h,K}, A_{\mathbf{n}_K}^{up} [z_h]_{F,K})_F. \end{aligned}$$

For boundary faces, one can use the symmetry of $A_{\mathbf{n}_K}^{up}$. □